

Lehigh University Lehigh Preserve

Theses and Dissertations

1-1-1983

Seismic damage and retrofit studies of the Mori-Sada building.

Shiunn-Jang Wang

Follow this and additional works at: <http://preserve.lehigh.edu/etd>



Part of the [Civil Engineering Commons](#)

Recommended Citation

Wang, Shiunn-Jang, "Seismic damage and retrofit studies of the Mori-Sada building." (1983). *Theses and Dissertations*. Paper 2367.

This Thesis is brought to you for free and open access by Lehigh Preserve. It has been accepted for inclusion in Theses and Dissertations by an authorized administrator of Lehigh Preserve. For more information, please contact preserve@lehigh.edu.

SEISMIC DAMAGE AND RETROFIT STUDIES

OF THE MORI-SADA BUILDING

by

Shiunn-Jang Wang

A Thesis

Presented to the Graduate Committee

of Lehigh University

in Candidacy for the Degree of

Master of Science

in

Civil Engineering

Lehigh University

May 1983

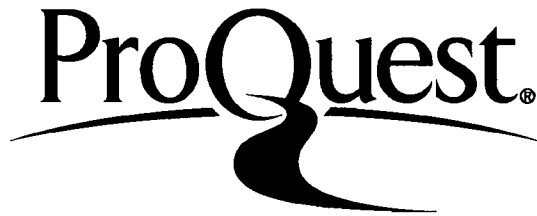
ProQuest Number: EP76643

All rights reserved

INFORMATION TO ALL USERS

The quality of this reproduction is dependent upon the quality of the copy submitted.

In the unlikely event that the author did not send a complete manuscript and there are missing pages, these will be noted. Also, if material had to be removed, a note will indicate the deletion.



ProQuest EP76643

Published by ProQuest LLC (2015). Copyright of the Dissertation is held by the Author.

All rights reserved.

This work is protected against unauthorized copying under Title 17, United States Code
Microform Edition © ProQuest LLC.

ProQuest LLC.
789 East Eisenhower Parkway
P.O. Box 1346
Ann Arbor, MI 48106 - 1346

CERTIFICATE OF APPROVAL

This thesis is accepted and approved in partial fulfillment of the requirements for the degree of Master of Science.

May 13, 1983
(Date)

Professor in Charge

Chairman of Department

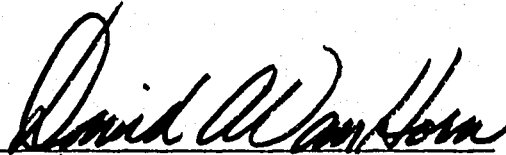
CERTIFICATE OF APPROVAL

This thesis is accepted and approved in partial fulfillment of the requirements for the degree of Master of Science.

May 13, 1983
(Date)



Professor in Charge



Chairman of Department

ACKNOWLEDGEMENT

It is a pleasure for the author to record his gratitude to Dr. Le-Wu Lu for his valuable guidance and encouragement during this study. The author also wishes to express his deep appreciation to Mr. Ching-Hwei Chue and Professor Matsui of Kyushu University for their help in translating the Japanese reports.

Special thanks are also due to Miss Christian C. Su for her help in drawing the figures. Sincere appreciation is also extended to Dr. Shosuke Morino in Kyushu University for providing much valuable information.

The research assistantship supported by the Fritz Engineering Laboratory of Lehigh University is sincerely appreciated.

Table of Contents

ABSTRACT	1
1. INTRODUCTION	3
1.1 Background	3
1.2 Objectives	5
1.3 Outline of Report	6
2. SEISMIC DAMAGE ANALYSIS OF THE MORI-SADA BUILDING	7
2.1 Description of the Building	7
2.2 Observed Damage	7
2.3 Previous Studies	8
2.4 Elastic Analysis	9
2.4.1 Modelling	9
2.4.2 Result and Discussion	11
2.5 Inelastic Analysis	12
2.5.1 DRAIN-2D Program	13
2.5.2 Modelling	14
2.5.3 Selection of Comparison Parameters	16
2.5.4 Result and Discussion	16
2.6 Summary	18
3. SEISMIC ANALYSIS OF THE MORI-SADA BUILDING RETROFITTED WITH CONCENTRIC AND ECCENTRIC BRACING SYSTEMS	20
3.1 General	20
3.2 Structure Selection	20
3.3 Design of Bracing Member	21
3.4 Models for Bracing Members	24
3.5 Modelling of Braced Frames	25
3.6 Lateral Stiffness per Unit Volume	26
3.7 Results and Discussion in Phase 1 Study	27
3.8 Results and Observations of Phase 2 Study	28
4. EFFECT OF ECCENTRICITY RATIO AND CONNECTION TYPE OF BRACING MEMBERS ON THE DYNAMIC RESPONSE OF THE RETROFITTED BUILDING	30
4.1 Introduction	30
4.2 System Selection	31
4.3 Modelling	32
4.4 Results and Observations	32
4.5 Discussion	34
4.6 The Effect of Eccentricity on Lateral Stiffness	36
4.7 Summary	37
5. CONCLUSIONS	39
TABLES	41
FIGURES	46

REFERENCES

63

VITA

66

ABSTRACT

A 4-story steel frame building, which is located in the downtown of Sendai, Japan and houses the Mori-Sada company, experienced a major earthquake in 1978 and suffered severe structural damage. In this report, elastic and inelastic analyses have been performed to investigate the causes of the damage. The calculated damage to structural members correlates well with the observed damage of the building. It is found that the major cause of the damage is the lack of lateral stiffness of the moment-resistant frame. The sudden change of column stiffness and the soft soil condition are also believed to be the contributing factors.

Different braced systems are introduced into the structure as a means of retrofitting the building. It is found that a vertical uninterrupted bracing system can make this building safer during further earthquakes. Also, a trend is observed that, in terms of increase in elastic stiffness per unit volume of bracing material, concentric K-bracing is more efficient than eccentrically K-bracing and concentric X-bracing systems, and pin-ended bracing is better than rigid-ended bracing.

A study of the effect of bracing eccentricity on the dynamic behavior of the retrofitted building with eccentric K braces is made. The results show lateral stiffness of the frame drops rapidly when bracing eccentricity increases. Hence, for the purpose of increasing lateral stiffness, the bracing eccentricity ratio should be kept as small as possible. Also, it is found that in terms of lateral stiffness rigid-ended bracing is more efficient than pin-ended bracing for bracing eccentricity ratios between 0.1 to 0.3.

1. INTRODUCTION

1.1 Background

On June 12, 1978, the Miyagi-Oki earthquake took place near the city of Sendai, Japan. It caused significant damage to the Mori-Sada building, whose structural system consists mainly of moment-resistant frames. The major damage was the plastic distortion in the columns of the third story of the building. Until now, no report has provided any clear explanation for the damages. The primary objective of this study are to investigate the reasons of the observed damages and to study the means of retrofitting the building.

By performing elastic and inelastic analyses of the Mori-Sada building, it is found out that the major cause of the damage is the lack of lateral stiffness characteristic of the moment-resistant frame. It is proposed to install some bracing members into the moment frame as the means of retrofitting the building. Three bracing systems, concentric K-bracing, eccentric K-bracing and concentric X-bracing systems, are adopted in the study.

The analyses of the retrofitted building with

different bracing systems show that concentric bracing can easily provide the needed lateral stiffness and it is more efficient than the eccentric bracing system so far as elastic behavior is concerned. However, the cyclic inelastic behavior of the concentrically braced frame is questionable. Many studies confirm that the cyclic inelastic behavior of concentrically braced frames is strongly influenced by the cyclic post-buckling behavior of the individual braces and its hysteresis loops is pinched and deteriorating [11, 14]. Previous research has shown that eccentrically braced frame is more reliable than concentrically braced frame in the inelastic range [15, 16]. For this reason, a detail study of the use of eccentric K-bracing system as a means of retrofitting the building is carried out. Instead of studying the design of the eccentric bracing member, the study emphasizes the effects of varying the amount of eccentricity and the connection types (pin connection vs rigid connection) on the dynamic response of the retrofitted building.

1.2 Objectives

The main objectives of this research are:

1. To study the elastic and inelastic dynamic response of the Mori-Sada building.
2. To provide a qualitative explanation of the observed column failure.
3. To study the dynamic response of the building with different bracing system; and to compare the performance of the retrofitted structure with that of the original structure. The bracing systems to be examined are
 - a. concentric X-bracing.
 - b. concentric K-bracing.
 - c. eccentric K-bracing.
4. To study the effect of varying the amount of eccentricity on the dynamic response of the retrofitted building with eccentric K-bracing members.
5. To study the effect of the different connection types of the bracing members on the dynamic response of the retrofitted building.

1.3 Outline of Report

Following Chapter 1, which gives an introduction to the study, this report presents the results of three separate, by coordinated, studies. In Chapter 2, elastic analysis and inelastic analysis of the original building are performed by using computer programs SAPIV and DRAIN-2D and explanations of the observed damage are provided. By installing different bracing systems into the original building, several retrofitted structures have been developed and analyzed. The results are presented in Chapter 3.

A series of inelastic dynamic analyses of the building retrofitted with eccentric K bracing are carried out in Chapter 4. The principal variables are the bracing eccentricity and the bracing connection. The bracing eccentricity varies from zero (concentric bracing) to 0.9 times the length of the girder of the braced bay. Two connection types, pin and rigid, are chosen. The results are given in Chapter 4. General conclusions of the study are presented in Chapter 5.

2. SEISMIC DAMAGE ANALYSIS OF THE MORI-SADA BUILDING

2.1 Description of the Building

The Mori-Sada building, which is located in Sendai, Japan, was completed in 1971. The building, shown in Fig.1, 2, and 3, is a 4-story office building, 7.3m x 13.3m in plan and 12.39m high, oriented with its longitudinal dimension in the N-S direction. It has three bays in the N-S direction and one bay in the E-W direction. The building has two full moment-resisting steel frames in the longitudinal direction, which is the weak direction of the columns. In order to increase the stiffness about the weak axis, two 9mm thick plates were welded to the wide flange columns in the first story (Fig. 4). All the other columns and girders are standard Japanese wide flange shapes. The member sizes of this structure are shown in Table 1.

2.2 Observed Damage

Because the earthquake ground motions are stronger in the N-S direction, the principal damages are found in the longitudinal moment-resistant frames. As shown in Fig. 5, there was a 1/15 permanent deflection in the third floor after the earthquake. The deformed shape of the columns in the third story is shown in Fig. 6. The

plastic deformation at the top and the bottom of the column is almost the same. Some cracks were found around the footings. Furthermore, the exterior wall on the third floor failed in shear and all the windows on the third floor were broken.

2.3 Previous Studies

There are several reports in Japanese containing information about this building. A check of design adequacy of this building has been carried out in Ref.

[10]. The results show that the design of this building satisfied all the requirements of the applicable Japanese code. Also, the quality of construction of this building has been investigated and found to be very satisfactory [3]. Furthermore, dynamic analyses with elastic material properties, shear building and lumped mass assumptions have been performed [1, 3, 10]. The energy method developed by Ben Kato [13] has been used in assessing the safety of the structure. In this method, the safety of a structure is evaluated by comparing structure's energy dissipating capacity with earthquake input energy. The results show that the energy concentration ratio is the highest between the second and third floor levels. The reports, therefore, conclude that the observed damage in the columns was due to the high

energy dissipation. However, no report offers any clearly explanation why the energy was so highly concentrated between these floors. Another suggestion is that it is the sudden change of the column stiffnesses at the second floor level that caused the problem [18]. But, no analytical study has been carried out to support this suggestion.

2.4 Elastic Analysis

There are two purposes of performing the elastic analysis in this study:

1. As a check for the correctness of the theoretical model by comparing the results obtained with the results presented in the Japanese reports.
2. As a check for the inelastic analysis results.

2.4.1 Modelling

SAPIV program [5] is used to perform the elastic analysis. Because the results of this analysis are used to be compared with the results of the previous studies, in which two dimensional planar frame models were used, the building is treated as two parallelal planar structures. The assumptions of the model used in this analysis are:

1. The foundation is infinitely rigid.
2. The structure is symmetrical in plan; hence, torsional deformation is neglected.
3. The girders provide all the flexural stiffnesses and any additional stiffness due to the floor slabs is ignored.
4. The structures are of the moment-resisting type and resist deformations only by the moments developed at the ends of the girders and columns.
5. Shear deformation in the girders and columns is neglected.
6. There is no extension (or contraction) between floors, since it is assumed that the structures are infinitely rigid in the vertical direction.
7. All masses are concentrated at the floor levels.
8. The mass of each floor moves horizontally. Vertical motion is not considered because of assumption 6. The rotational inertia associated with each joint is considered.

The node and element numbering adopted in the analysis is shown in Fig. 7. The three-dimensional beam elements are

used for the beams and columns. The mode superposition method is used in the time-history analysis. The E-W direction, 25 seconds earthquake record obtained from the strong motion instruments installed in the Architectural and Civil Engineering building of the Tohoku University in Sendai is used as the base excitation [19].

2.4.2 Result and Discussion

The natural period of the building computed by SAPIV was 1.05 second which is very close to the natural period 1.12 second given in Ref. [1]. This comparison provides some confidences in the results of this analysis.

A plot of the maximum story drift of each floor is shown in Fig. 8 and the maximum bending moment in the columns are listed in Table 2. It is shown that the moments in some columns exceeded the plastic moments very early during the earthquake. Inelastic behavior therefore occurred in the structure soon after the earthquake had begun. The results of the elastic analysis of course are no longer valid after initial yielding.

2.5 Inelastic Analysis

The results of the elastic analysis clearly indicated that the behavior of the building during the earthquake is far from being elastic. The purpose of performing the inelastic analysis in this study is to understand the true behavior of the building during the earthquake in order to find out the reason for the observed damages.

There are three different sizes of columns in this building and they are designated as Section 1 for the columns of the first story, Section 2 for the second story, and Section 3 for the third and fourth stories. As mentioned in the previous section, it has been suggested that the change of the column stiffness at the second floor level may have caused the energy concentration. To verify this, four structures with varying column sizes have been developed and analyzed by the DRAIN-2D program. The descriptions of these four structures and the reason to develop them are stated as follows:

1. System 1 -- The original Mori-Sada building.
2. System 2 -- Changing the size of columns in the second story from Section 2 to Section 1.

The motive is to increase the stiffness change at the floor level 2, which may cause an increase in the energy concentration.

3. System 3 -- Changing the size of the columns on the third story from Section 3 to Section 2. The idea is to eliminate the stiffness change at the second floor level.
4. System 4 -- Including changes in both System 2 and System 3.
5. System 5 -- Using Section 1, the strongest section, for all the columns to eliminate the column stiffness change. The purpose of this system is to investigate the ability of the moment frame to resist lateral load.

2.5.1 DRAIN-2D Program

DRAIN-2D is a general purpose computer program for the inelastic response of planar structures subjected to earthquake ground motions. The program concepts and features are described in Ref. [12]. The structure is idealized as a planar assemblage of discrete elements. Analysis is done by the Direct Stiffness Method, with the nodal displacements as the unknowns. Each node possessed

up to three displacement degrees of freedom, as in a typical plane frame analysis. The analysis uses a step-by-step procedure with the yield state of each element checked at the end of each time step. The tangent stiffness modifications and the equilibrium corrections for any imbalance due to changes in state are applied at the end of each time step. The time step is held constant, and no iteration is used.

2.5.2 Modelling

The node and element numbering adopted in this analysis is the same as that in the elastic analysis (Fig. 7). The following points may be noted:

1. Masses are associated only with the horizontal and rotational displacement at the floor levels.
2. Beam-column elements are used throughout for every member.
3. Each girder is represented by a single element so that plastic hinges may form at the girder ends only.
4. Element lengths from center to center of joints have been assumed throughout.
5. P-M interaction is taken into account for the

- columns, assuming interaction surfaces as for steel I-sections (Fig. 9).
6. A strain hardening ratio of 5% is assumed for all element.
 7. The P- Δ effect is taken into account by adding geometric stiffness to the column stiffness.
 3. All the structures are analyzed with the original stiffness-proportional damping, which is assumed to be equal to 5% of the critical damping for the first mode. The original stiffness-proportional damping is chosen because it is felt to be more indicative of the true conditions [15]. Also, it distributes the damping effect throughout the structure and not just at the mass points.
 9. All the analyses are performed with a 0.01 second time step, which has been chosen after several trial runs. Considerable inelastic activity occurs during this time span, and the results with this time step are sufficiently similar to the results with a smaller (0.005 seconds) time step.
 10. A yield stress of 2500 kg/cm² is assumed

throughout the study.

2.5.3 Selection of Comparison Parameters

Instead of using ductility ratio to express the ductility demands on the structural members, the DRAIN-2D program provides values of the total plastic deformations, which are believed to be more meaningful physically than those rather artificial ratio [12]. Those total deformations are computed as indicated in Fig. 10, by accumulating the plastic rotation during all positive and negative plastic excursions. In this study, the maximum story drift and maximum total plastic hinge rotation of columns on each floor are chosen to be the parameters for comparison.

2.5.4 Result and Discussion

The maximum total plastic hinge rotations of the stories are shown in Fig. 11 and maximum story drifts are shown in Fig. 8. The plastic deformations concentrate at the columns of the third story where severe column damage occurred. The calculated damage to the structural members seem to correlated well the actual damage of the building. However, the permanent deflection of the third floor level computed by DRAIN-2D after 25 second earthquake excitation is 10cm which is smaller than the

observed damage, 13cm. It has been reported in Ref. [10] that the building rests on a soft soil, which was previously a rice field. Ref. [17] reports that the deep layers of the relatively soft soil are particularly dangerous for the building because of their acceleration amplification characteristics. Hence, it is believed that the infinitely rigid foundation assumption may be the reason for the difference between predicted result and observed damage. Another factor is that the ground motion record used in the analysis is not obtained from the same building.

The results for System 2 indicate that the increase of the column size of the second story tends to increase the damage in the third story. Furthermore, the damage mechanism is changed in System 3, in which the major damage occurs at the columns on the second story instead of the third story. In this system, the column stiffness changes at the first floor level. From these two observations, a trend that the energy dissipation tends to concentrate on the floor where the column stiffness changes may be established.

The most interesting finding is in the response of System 5. This system is supposed to be a very safe

structure because every column in this system has double, even triple, flexural stiffness than the corresponding column in the original structure. However the analysis results show that the story drift control of this system is not improved very much. Moreover, the plastic hinges are found at the first floor. It indicates that neither the increase of column flexural stiffness nor avoiding the column stiffness change can improve this building. Hence, the energy concentration are not the major reasons for the damage. The real problem is that the lateral stiffness of the moment frame is too low. The excessive deflection developed during the earthquake because of the low lateral stiffness and the resulting increase in the P- Δ effect caused high stresses and plastic deformation in the columns.

2.6 Summary

By performing elastic dynamic analysis on the moment frame of the original building and inelastic dynamic analyses on the building and its four modifications, the reasons for the damages can be noted as follows:

1. The moment-resisting frame produced excessive deflections due to the lack of lateral stiffness. This excessive deformation

increases the P- Δ effect, which in turn increases the stresses in members and causes the plastic deformations.

2. The sudden change of column stiffness at the second floor level causes the damages to be concentrated in the third story.
3. The soft soil under the building possibly amplified the input acceleration and increased the damage.
4. The building was designed by the weak column - strong beam design concept. That is the reason why the plastic hinges formed only in the columns.

3. SEISMIC ANALYSIS OF THE MORI-SADA BUILDING RETROFITTED WITH CONCENTRIC AND ECCENTRIC BRACING SYSTEMS

3.1 General

Since the main problem of the Mori-Sada building is the weak drift control characteristic of the moment-resistant frame, it is proposed to investigate how the performance of the building can be improved by installing an internal bracing system.

This study consists of two phases. The first phase is to investigate the behavior of the bracing systems with different arrangements of bracing members in a concentric X-bracing system. The second phase is to study the behavior of the structures with different bracing systems. The bracing systems included are the concentric X-bracing, concentric K-bracing and eccentric K-bracing systems.

3.2 Structure Selection

In the first phase, in which the behavior of the structures with different arrangements of bracing members are investigated, only concentric X-braced frames are studied. Five systems have been chosen and are shown in Fig. 12. In the second phase, two different sizes and

two different connection types of the braces are considered. The structures used in this phase of study are shown in Fig. 13, Fig. 14, and Table 3.

3.3 Design of Bracing Member

The seismic lateral design forces are taken as specified by the Uniform Building Code [20]. According to this code the design base shear is

$$V = ZIKCSW \quad (3.1)$$

where W is the total dead load and applicable portions of other load, which has been taken to be full live load in this study. The numerical coefficient C is determined from $C = 1/15T$, where T = the fundamental elastic period of the structure and suggested by the code as $T = 0.05 H/D$. (H/D is the height-to-width ratio of building) The site resonance factor S depends on the ratio of building period T to characteristic site period T_s . In this study, S is taken as 1.5. The code also specifies that the product CS need not exceed 0.14 and therefore is taken to be 0.14. The coefficients Z , I and K are taken as 1. As required by the code, all bracing members in the braced frame are designed for 1.25 times the force determined from Equation 3.1.

The following formulas presented in Ref. [4] for designing diagonal tension bracing members are used.

Design Condition 1: Lateral Stiffness Under Working Loads.

$$A_b = \frac{F_b L_b^2}{EL\Delta - \sigma_g L^2 - Ee_c h} \quad (3.2)$$

in which

E = modulus of elasticity;

F = tension force in bracing member due to lateral loads plus $P-\Delta$ shear;

e = sum of elongation of columns due to lateral loads plus $P-\Delta$ shear;

σ_g = axial compressive stress in beam due to lateral loads plus $P-\Delta$ shear; and

Δ = $0.002h$

L = length of bracing member;

L_o = length of braced bay

h = height of the braced bay.

Design Condition 2: Strength and Stability Under Design Ultimate Loads.

Strength Requirement:

$$A_b = \frac{L_b}{0.85\sigma_y L} \Sigma H + \frac{L_b^3}{EhL^2} + \frac{L_b \sigma_g}{0.85\sigma_y Eh} + \frac{L_b e_c}{0.85\sigma_y L^2} \Sigma P_1 \quad (3.3)$$

in which

ΣH = story shear due to the applied lateral loads (L.F. = 1.30);

ΣP_1 = total applied gravity load above the story which contributes to the P shear in the story (L.F. = 1.30).

σ_y = yield stress level of the diagonal brace. All other terms have been defined previously.

Stability Requirement:

$$A_b = \frac{L_b^3}{EhL^2} + \frac{L_b \sigma_g}{0.85\sigma_y Eh} + \frac{L_b e_c}{0.85\sigma_y L^2} \Sigma P_2 \quad (3.4)$$

in which ΣP_2 = total gravity load above the story which contributes to the shear in the story (L.F. = 1.70). All other terms have been defined previously.

Design Condition 3: Brace Slenderness Requirement.

$$r_b \geq L_e / 300 \quad (3.5)$$

in which r_b is the radius of gyration of the bracing

member and L_e is the effective length of the diagonal brace between points of support, as defined in the AISC Specification [2]. The above formula provide the minimum area for the bracing member. Although these procedures are recommended only for concentric X-braced frames, in order to compare the performace of different bracing systems, the same bracing member are used for other bracing systems. After performing the calculations metionsed above, the equal leg single angle section 75x75x9 (Japanese shape) and the double angle section 3x3x3/8 (US shape) are chosen. The latter has almost twice the stiffness of the first one. The reason for choosing two different sections is to investigate the effect of bracing member size on the behavior of the structure.

3.4 Models for Bracing Members

In the past studies of braced frames, the hysteresis behavior of primarily axially loaded bracing members has been modeled in one of the several ways, such as: elastic in tension and compression, tension-only elastic model, tension-yield and compression-yield, or tension-yield and compression-buckling. These models neglected the energy dissipation characteristics of bracing members in the post-buckling range. In Ref. [8], Jain presented

a hysteresis model which accounts for the energy dissipation characteristics of bracing members. This model has been incorporated with the DRAIN-2D program as Buckling Element EL9 [9]. This element type is used as the model of pin-ended bracing member. Another model, End Moment-Buckling Element (EL10), which is a combination of buckling element (EL9) and beam-column element (EL2) is used as the model of rigid-connected bracing member.

3.5 Modelling of Braced Frames

The node and element numbering for the braced systems used in this study is shown in Fig. 13 and Fig 14. The following points may be noted with regard to modelling:

1. All the modelling for the moment frame remain the same as described in Chapter 2.
2. Buckling element (EL9) is used for pin-ended bracing member. End moment-buckling element (EL10) is used for rigid-connected bracing member.
3. The maximum compressive load was assumed to be the Euler's buckling load.
4. The cycling load (P_{ync}), equal to $25/(L/r)$ times the yield load.

5. Time step 0.01 is used.
6. The first 5 seconds of the Miyagi-Oki earthquake record are used in order to reduce computer time.
7. Because the shear force in the link of an eccentric bracing system is very large, there is a great possibility that the link may fail in shear. In order to consider this mode of failure, the plastic moment M_p of the link is taken as the smaller value of the normal plastic moment of the link and the end moment when the link fails in shear. The latter is computed as the yield force times the length.
8. The eccentricity ratio (e/L) is 0.1 for the eccentric K-bracing system.

3.6 Lateral Stiffness per Unit Volume

In order to compare the performance of different bracing systems, the lateral stiffness per unit volume, which is the total lateral stiffness divided by the volume of the member, is introduced. The lateral stiffness is defined as the total base shear divided by the maximum lateral deflection at the top of the structure. The lateral stiffness per unit volume of a braced structure is used to show the efficiency of using

various bracing systems.

3.7 Results and Discussion in Phase 1 Study

The responses of the structures in phase 1 are given in Table 4. First of all, the damages in System 4 and 5 are found in the columns in the second floor and are worse than the observed and evaluated damages of the original structure. This indicates that installing bracing members in the third story or in the third and fourth story would only strengthen the floors being braced and would cause damages to occur in the unbraced floors. This observation is very similar to what was found in Chapter 2.

The results also show that there are no plastic hinges in the first three systems which have uninterrupted vertical bracing systems. Furthermore, the bending moments in the columns in the third story of these systems are only half of those in the original structure and the maximum story drifts are only one fifth of those in the original structure. These observations show that the performance of the building can be significantly improved by installing a continuous bracing system.

Comparing the story drifts and bending moments in the columns of these systems, it is found that the bracing in the larger bay offers more story drift control, yet does not increase the maximum moment in columns. Another way of comparing bracing performance is to examine the lateral stiffnesses per unit volume provided by the bracing systems. They are given in Table 5. It may be seen that System 3 has the highest stiffness per unit volume and is the most efficient system.

3.8 Results and Observations of Phase 2 Study

Nine systems (Table 3) have been analyzed in this phase of study. Their responses are shown in Table 6. The lateral stiffness per unit volume for each system is computed and listed in Table 6. The observations that may be made from this phase of study are as follows:

1. The behavior of all the bracing systems are within elastic range. No plastic hinge is found in any system. This shows that a vertical uninterrupted bracing system can make this building safer for similar earthquake.
2. When only the elastic behavior is considered, concentric K-bracing system is more

efficient than concentric X-bracing and eccentric K-bracing systems.

3. When using the same brace size, concentric X-bracing system provides more story drift control than other bracing systems. On the other hand, pin-ended bracing provides less story control than rigid-ended bracing.
4. Increasing the bracing size seems can increase the lateral stiffness per unit volume and more story drift control can be gained.

efficient than concentric X-bracing and eccentric K-bracing systems.

3. When using the same brace size, concentric X-bracing system provides more story drift control than other bracing systems. On the other hand, pin-ended bracing provides less story control than rigid-ended bracing.
4. Increasing the bracing size seems can increase the lateral stiffness per unit volume and more story drift control can be gained.

4. EFFECT OF ECCENTRICITY RATIO AND CONNECTION TYPE OF BRACING MEMBERS ON THE DYNAMIC RESPONSE OF THE RETROFITTED BUILDING

4.1 Introduction

It is shown in Chapter 3 that the concentric bracing member is more efficient than eccentric bracing member in the elastic range. However, many studies have shown that the eccentric bracing member is more reliable in inelastic behavior than the concentric bracing member [15, 11]. Hence, a study on the eccentric bracing system is carried out in this Chapter.

The basic characteristics of an eccentrically braced frame may be noted by examining the elastic as well as plastic behavior of a simple diagonally braced frame [6] , such as shown in Fig. 15. The dependence of the elastic frame stiffness on the parameters e/L is illustrated in Fig. 15. By varying the ratio e/L from 0 to 1, the frame changes in character from a concentrically braced frame to a conventional moment-resisting frame. For all intermediate values of e/L , the frame becomes eccentrically braced. The curve clearly shows the advantages of bracing the frame to gain lateral

stiffness in the system.

It has been noted by Hjelmstad that the results shown are only for a one-story frames and that the member boundary conditions in one-story frames are different from those found in multistory frames [6]. As an extension of the Hjelmstad's study, the effect of the eccentricity ratio and connection type on the dynamic response of multistory frame are investigated, using the Mori-Sada building as the skeleton structure.

4.2 System Selection

Theoretically speaking, eccentrically braced frames is designed by the plastic methods, where the force distribution is determined by a lower bound moment balancing technique [7], with the lateral loads determined by an applicable building code. Since in this study only the effects of changing eccentricity ratio and connection type are examined, it is appropriate and convenient to use the girders and columns of the original building and one of the bracing sizes adopted in Chapter 3, the double angle 3x3x3/8. By varying the eccentricity ratio from 0 to 0.9, 20 structures with the same member sizes are analyzed by the DRAIN-2D program.

4.3 Modelling

All the input parameters are the same as those used in chapter 3. In order to study the inelastic behavior of the retrofitted buildings, 1.5 times the Miyagi-Oki earthquake record is used as the base excitation.

4.4 Results and Observations

The 20 structures analyzed are divided into two groups. Group 1 contains 10 systems with pin-ended bracing member and group 2 contains 10 systems with rigid-ended bracing member. The results of analyses are present in Fig. 16, 17, 18 and Table 7. The following observations have been made during the course of the investigation and from the computer results.

1. As shown in Fig. 16, the maximum horizontal story drift of the frame increases as the bracing eccentricity increases. This means that an increase in the eccentricity tends to reduce the stiffness of the structures. This will be discussed in more detail later.
2. All the bracing element in the group 1 structures did not fail in tension. However, 3 structures in group 2 did have bracing failure. The results also show that higher

axial forces would be presented in rigid-ended bracing members than in pin-ended bracing members.

3. Shear link failure are found in group 2. Nine links fail in the structure with $e/L=0.6$, two with $e/L=0.7$ and three with $e/L=0.8$. These three structures happen to have bracing failure also. It was first believed that the link failure may be related to the failure of the bracing members. But, it was later found that the stress imbalances at the eccentric nodes and the vertical displacements at these nodes were unreasonable. This problem will be investigated and discussed in detail in a later section.
4. As shown in Table 7, the maximum accumulated plastic hinge rotations of both beams and columns increase with increasing eccentricity. This is another indication that increase in bracing eccentricity tends to decrease the stiffness of the structure. However, it is observed that all the maximum plastic hinge rotations occur on the columns of the third floor. So, the damage mechanism of the

retrofitted frame with various bracing eccentricities would be the same as in the original moment-resisting frame.

4.5 Discussion

As mentioned in Section 4.4, the member forces and the vertical displacements of the failed link appear to be unreasonable. The member forces do not satisfy equilibrium at the eccentric nodes and the vertical displacements are too large. It is felt that a detailed study is necessary to provide an explanation for the problem.

The same subject has been investigated by Roeder and Popov [15]. Their suggestion is that it is due to the use of original stiffness-proportional damping. This damping property is also used in this study because it predicts a more realistic distribution of the damping effects and does not lead to a decrease in damping after member yielding. It also offers more computational stability in the analysis.

The DRAIN-2D computer program handles this type of damping by augmenting the structural stiffness at the start of the analysis and adding a load term at the end

of each time step throughout the analysis [12]. The load term is added to the unbalanced load vector, which includes unbalanced loads due to change of yield state, as the corrections for the nonlinearities of the system. The unbalanced load vector is then added to the next time step, because no iteration is performed within the time step. By carefully examining the results, the imbalance and large vertical displacement did not start until the eccentric element started to exhibit large amounts of yielding. Before the eccentric member yields, the vertical velocities of the eccentric nodes are zero. However, after a bracing yields, the vertical velocity of the eccentric node becomes very large. These large vertical velocities produce large damping loads to be added to the bracing nodes after each time step. Eventually, it is these large vertical damping loads that lead to extra stresses in the link and cause it to fail. It is thus confirmed that the imbalance in member forces is caused by the application of a load through the unbalanced load vector used in the computer program.

It is therefore apparent that the predicted link failure may not be realistic and the results should not be included in the comparison study. However, the story drift and the base shear of the entire structure have not

been affected very much by the local link failure and it is felt that they can be used as a rough indication of the stiffness of the structure in the study.

4.6 The Effect of Eccentricity on Lateral Stiffness

In this section, the variation of lateral stiffness of the retrofitted frame with eccentric K bracing frame is discussed. As defined in Chapter 3, the lateral stiffness of the braced frame can be computed as the total base shear divided by the lateral deflection at the top of the structure. The total base shear can be computed by summing up the maximum shear forces in the columns on the first floor. The base shears of the systems in this study have been computed and are shown in Fig. 17. The base shear is maximum when $e/L=0.6$ for the case of pin-ended bracing and when $e/L=0.7$ for rigid-ended bracing.

The stiffness terms are normalized dividing the calculated stiffness by the stiffness of the original frame retrofitted with concentric bracing, (i.e. eccentricity equals zero). The results are shown in Fig. 18. Once again, it may be observed that the stiffness decreases as the eccentricity increases. For eccentricity ratios greater than about 0.5, the lateral

stiffness for both pin-ended and rigid-ended bracing systems decreases rather slowly. This means that for large bracing eccentricities, the type of connection has only a small effect on the lateral stiffness. On the other hand, when the eccentricity is small ($e/L < 0.2$), the rigid-ended bracing systems have 40% more lateral stiffness than the pin-ended bracing systems.

For rigid-ended bracing system, stiffness drops considerably when e/L is greater than 0.2. For pin-ended bracing system, stiffness drops rather rapidly between $e/L=0.1$ and $e/L=0.3$. This shows that in eccentrically braced frames rigid-ended bracing system would be more efficient than pin-ended bracing system in improving lateral stiffness in e/L ratio smaller than about 0.3.

4.7 Summary

The results of this study may be summarized as follows:

1. The maximum story drifts and the maximum accumulated plastic hinge rotations of the retrofitted structures would increase as the bracing eccentricity increases. On the other hand, the lateral stiffness of the retrofitted

structure would decrease as the bracing eccentricity increases. Hence, for the purpose of increasing lateral stiffness, the ratio e/L should be kept as small as possible.

2. Base shear is maximum when $e/L=0.6$ for the case of pin-ended bracing and when $e/L=0.7$ for rigid-ended bracing cases.
3. Lateral stiffness is not sensitive to bracing eccentricity when $e/L > 0.5$.
4. Pin-ended bracing systems lose more stiffness than rigid-ended systems for e/L ratio between 0.1 and 0.3. Also within this range of e/L ratio, rigid-ended bracing system is more efficient in improving lateral stiffness than pin-ended bracing system.
5. By using original stiffness-proportional damping property, the DRAIN-2D program would provide unrealistic link failure when a bracing member yields. This is caused by the application of load through the unbalanced vector used in the computer program.

5. CONCLUSIONS

The major conclusions of this study are:

1. The principal cause for the damage of the Mori-Sada building is the lack of lateral stiffness of the moment frame in the longitudinal direction. The sudden change of column stiffness and the soft soil condition probably also contributed to the damage.
2. A trend that the energy dissipation tends to concentrate on the floor where the column stiffness changes is observed.
3. By introducing a vertical uninterrupted bracing system, the building could considerably perform better in further earthquakes.
4. If concentric X-bracing system is used to retrofit the building, a vertical uninterrupted bracing in the longest bay is more efficient than other arrangements.
5. When only the elastic behavior is considered, concentric K-bracing system is more efficient than concentric X-bracing and eccentric K-bracing systems.
6. When using the same brace size, concentric

X-bracing system provides more story drift control than other bracing systems. On the other hand, pin-ended bracing provides less story control than rigid-ended bracing.

7. If eccentric K-bracing system is used, the maximum story drifts and the maximum accumulated plastic hinge rotations of the retrofitted structures would increase as the bracing eccentricity increases. Also, the lateral stiffness of the retrofitted structure would decrease as the bracing eccentricity increases. Hence, for the purpose of increasing lateral stiffness, the ratio e/L should be kept as small as possible. On the other hand, pin-ended bracing systems lose more stiffness than rigid-ended systems for e/L ratio between 0.1 and 0.3. Also within this range of e/L ratio, rigid-ended bracing system is more efficient in improving lateral stiffness than pin-ended bracing system.

TABLES

Table 1 Member Sizes of the Building

Type	Designation	Size
Column	C1	H-300x300x10x15 (2 9mm plates welded)
Column	C2	H-300x300x10x15
Column	C3	H-250x250x9x14
Girder	G1	H-294x200x8x12
Girder	G2	h-244x175x7x11
Girder	G3	H-336x249x8x12
Girder	G4	H-294x200x8x12

Table 2 Maximum Bending Moment in Columns Computed by SAPIV

Column No.	Max Moment (kg-cm)	Plastic Moment (kg-cm)	Estimated Time to Reach Plastic Moment
1	3.132×10^6	2.168×10^6	3.15sec
2	3.372×10^6	"	3.15 sec
3	3.54×10^6	"	3.15 sec
4	3.122×10^6	"	3.15 sec
5	1.527×10^6	1.125×10^6	3.7 sec
6	2.252×10^6	"	3.1 sec
7	2.474×10^6	"	3.1 sec
8	1.84×10^6	"	3.1 sec
9	1.359×10^6	7.3×10^5	3.1 sec
10	1.977×10^6	"	3.1 sec
11	2.15×10^6	"	3.1 sec
12	1.634×10^6	"	3.1 sec
13	8.07×10^5	"	11.3 sec
14	1.286×10^6	"	3.25 sec
15	1.406×10^6	"	3.15 sec
16	1.011×10^6	"	10.85 sec

Table 3 Systems in Phase 2 Study of Chapter 3

System	No.1	No.2	No.3	No.4	No.5	No.6	No.7	No.8	No.9
Bracing Type	X	X	X	K	K	K	E	E	E
Connection Type	F	S	F	F	S	F	F	S	F
Section No.	1	1	2	1	1	2	1	1	2

X: Concentrical X-bracing.

K: Concentrical K-bracing.

E: Eccentrically K-bracing.

F: Rigid-ended.

S: Pin-ended.

Section 1: 75x75x9 (Japanese shape)

Section 2: Double angle 3x3x3/8 (US shape)

Table 4 Responses of Systems in Phase 1 Study of Chapter 3

System No.	Max Story Drift (cm)	Max Plastic Hinge Rotation (radius)
1	3.9	0.
2	3.3	0.
3	3.5	0.
4	9.35	0.0316
5	8.7	0.03
Mori-Sada Building	13.86	0.029

Table 5 Comparison among Three Arrangements of Bracing Systems

	System 1	System 2	System 3
Base Shear (kg)	24998	23828	23899
Max Story Drift (cm)	3.9	3.5	3.3
Lateral Stiffness (kg/cm)	6410	6808	7242
Lateral Stiffness per Unit Volume (kg/cm ⁴)	6.536×10^{-3}	7.23×10^{-3}	7.69×10^{-3}

Table 6 Reponse of Systems in Phase 2 of Chapter 3

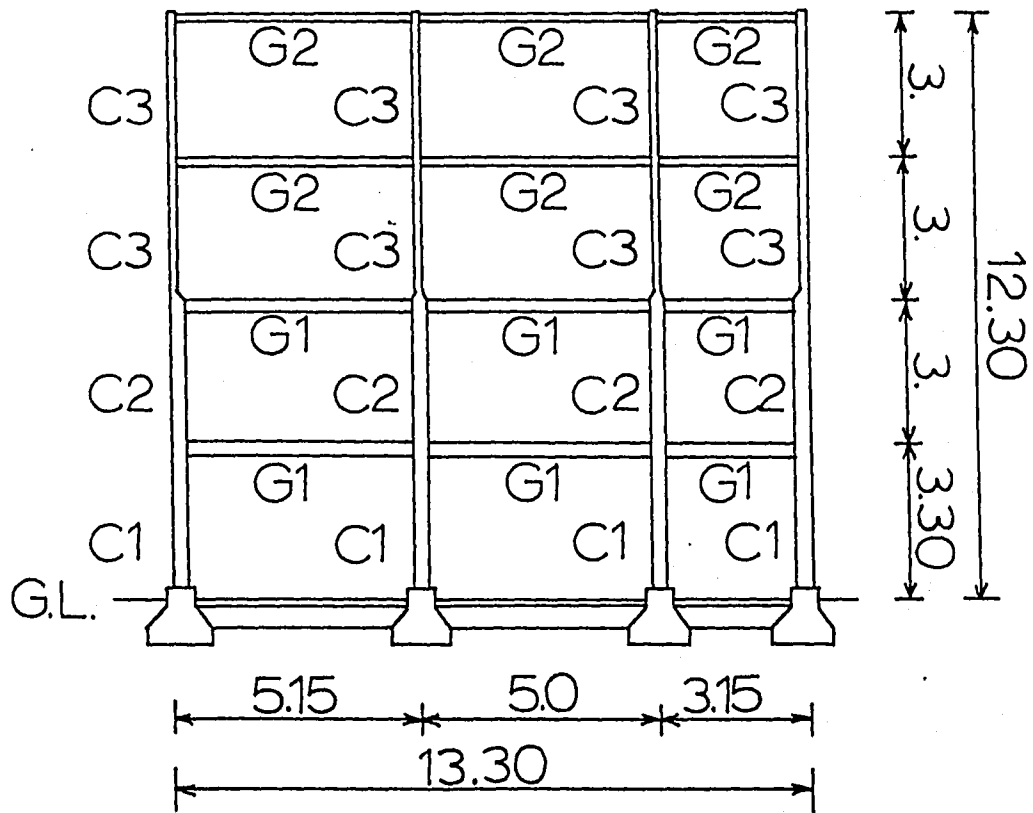
System No.	Max Moment in Column (kg-cm)	Max Moment in Beams (kg-cm)	Base Shear (kg)	Max Story Drift (cm)	Lateral Stiffness per Unit Volume (kg/cm ⁴)
1	1309350	921983	23075	3.5	0.00672
2	1417204	991893	24272	3.57	0.00693
3	1563593	941428	23858	2.7	0.00732
4	1687915	1305945	29331	4.0	0.00712
5	1701547	1555320	29331	4.1	0.00736
6	1817830	1637250	28390	3.4	0.00826
7	2073915	1856746	36869	6.73	0.0056
8	2003112	1763541	36892	6.69	0.0056
9	1185054	1177899	22114	3.7	0.0058

Table 7 Maximum Plastic Hinge Rotations of Systems
in Chapter 4

e/L	Pin-ended		Rigid-ended	
	Max Plastic Hinge Rotation in Columns (radius)	Max Plastic Hinge Rotation in Beams (radius)	Max Plastic Hinge Rotation in Columns (radius)	Max Plastic Hinge Rotation in Beams (radius)
0.	0.00125	0.00333	0.0016	0.00096
0.1	0.00722	0.00435	0.00619	0.00401
0.2	0.00754	0.0056	0.00283	0.00524
0.3	0.01486	0.00756	0.00788	0.00892
0.4	0.02664	0.0064	0.0208	0.01586
0.5	0.0268	0.01586	0.0301	0.01633
0.6	0.02925	0.0142	0.08	89. ¹
0.7	0.02914	0.01437	0.04	85. ¹
0.8	0.04	0.00541	0.06	141. ¹
0.9	0.05	0.00855	0.0414	0.01203

¹Link failure caused by the application of a fictitious load through the unbalanced load vector used in DRAIN-2D program. See Section 4.5.

FIGURES



DIMENSION (M)

Fig. 1: N-S Direction View of the Building

FIGURES

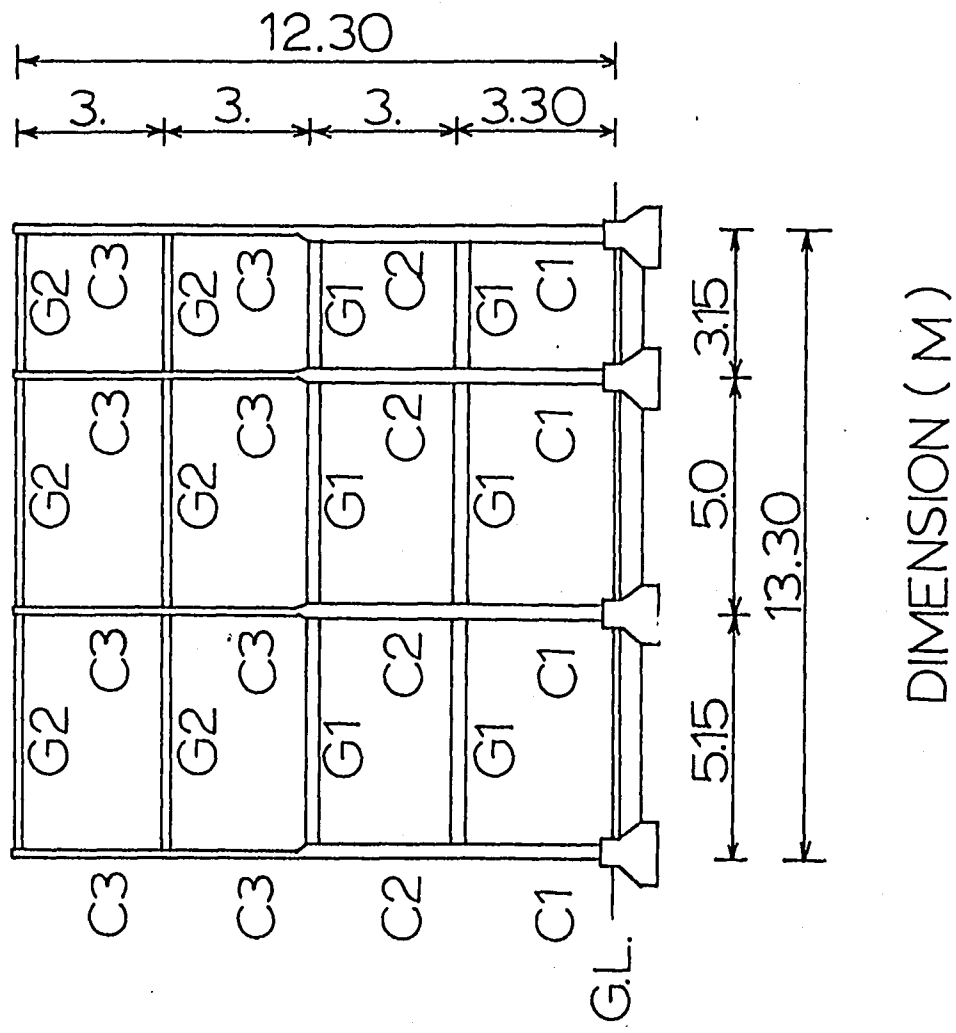


Fig. 1: N-S Direction View of the Building

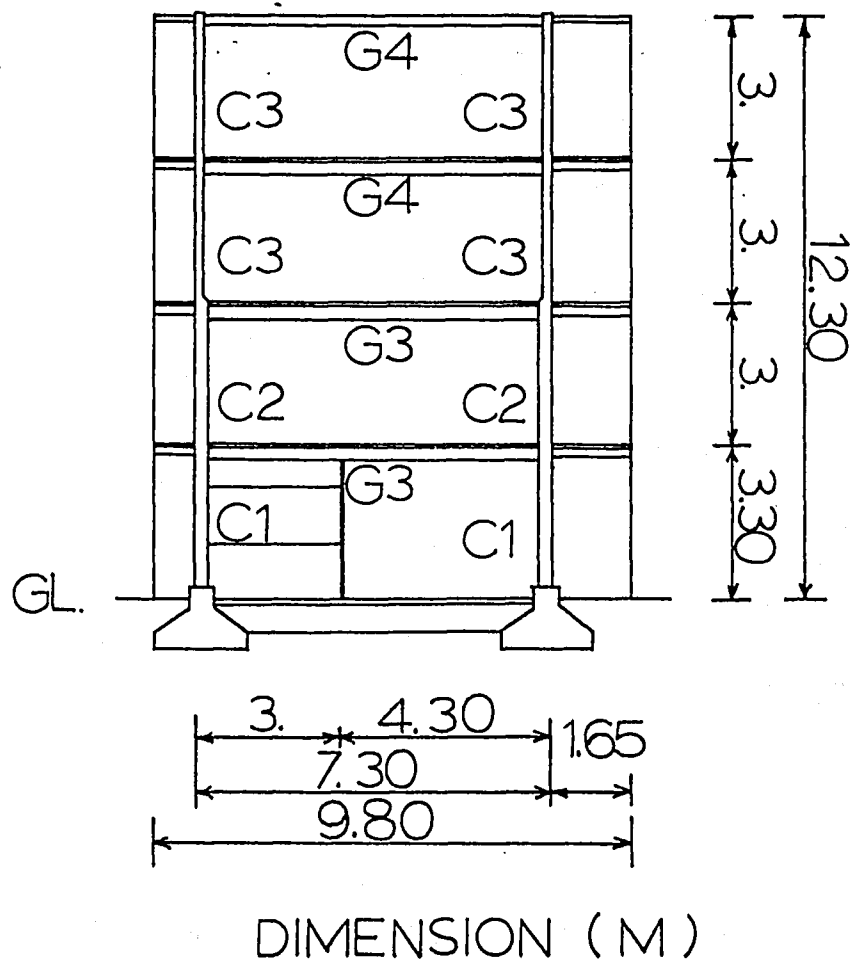


Fig. 2: E-W Direction View of the Building

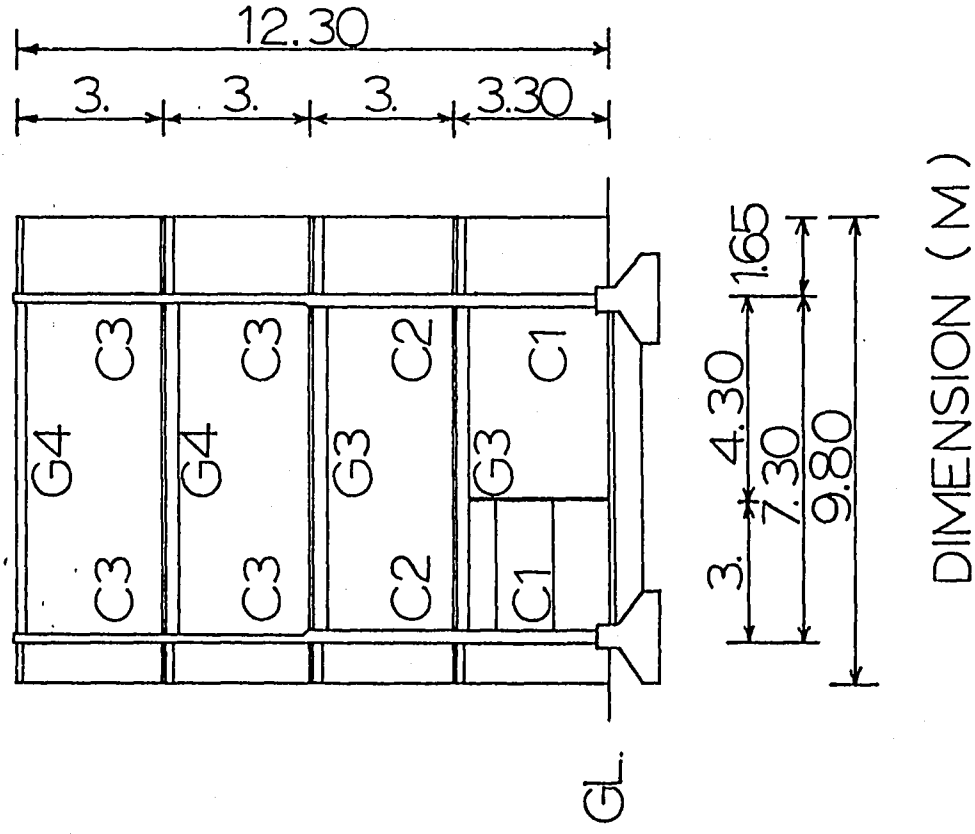
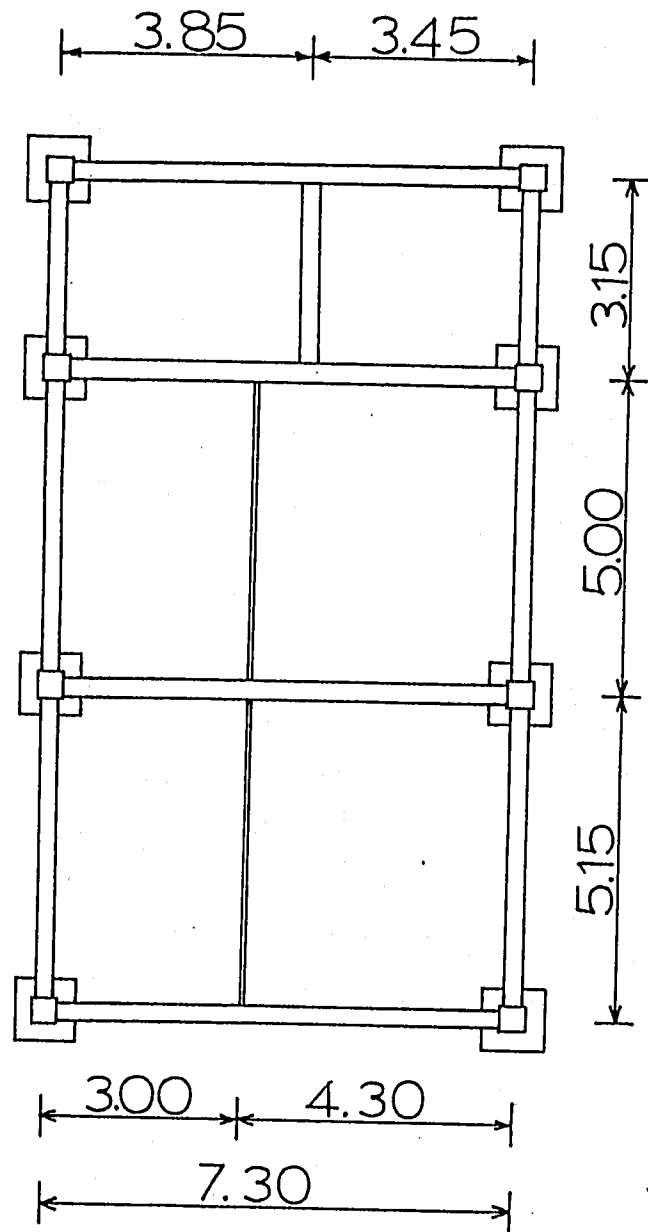
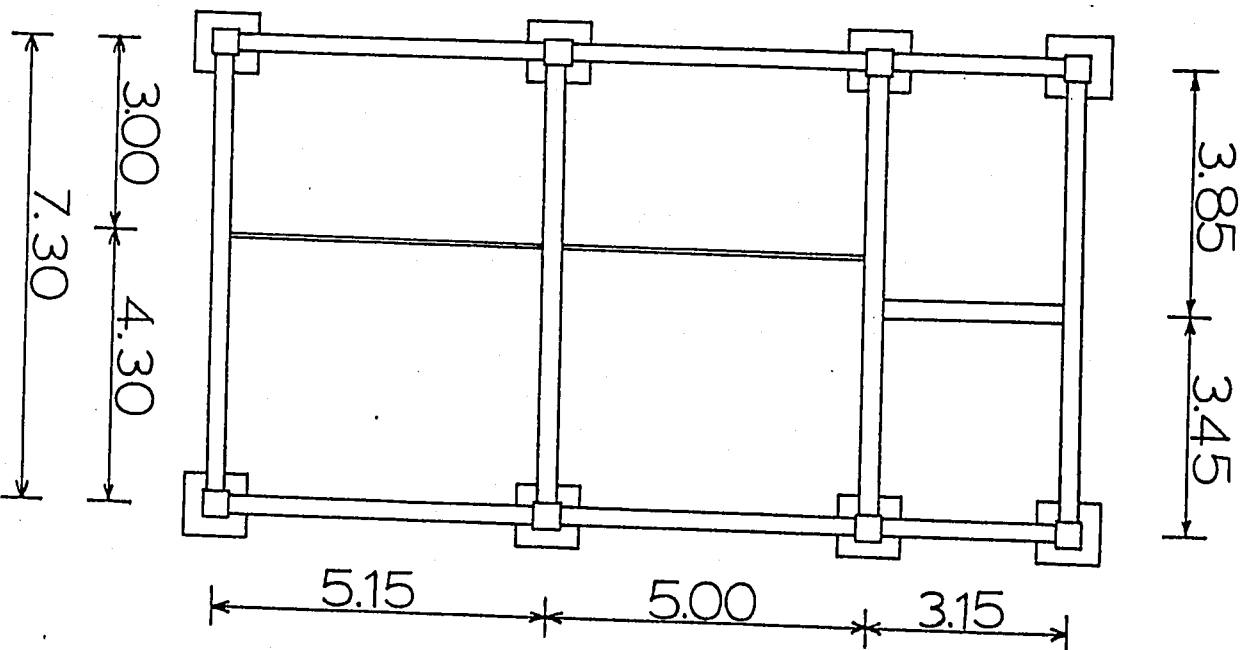


Fig. 2: E-W Direction View of the Building



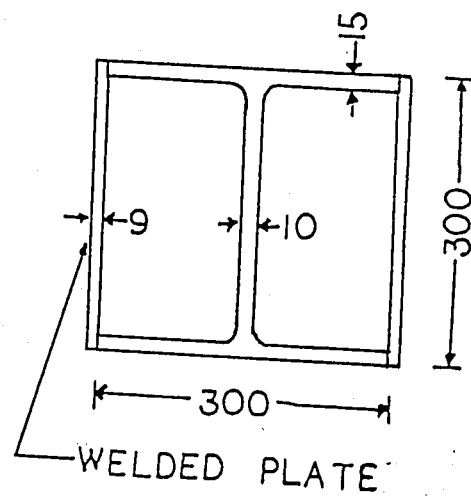
DIMENSION (M)

Fig. 3: Floor Plan of the Building



DIMENSION (M)

Fig. 3 : Floor Plan of the Building



* DIMENSION IN MM

Fig. 4: Column Cross Section in First Story

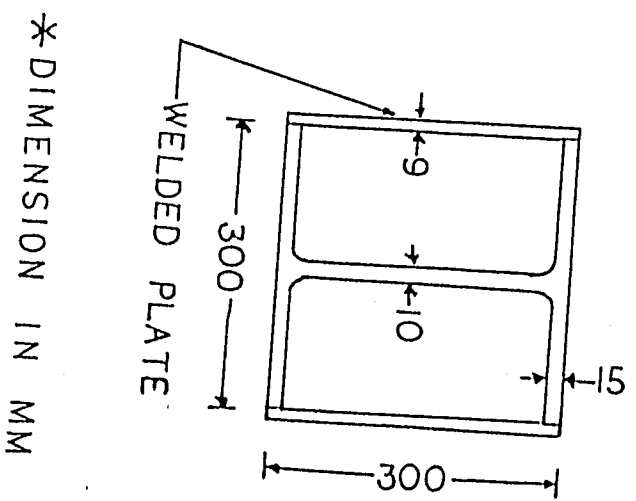


Fig. 4: Column Cross Section in First story

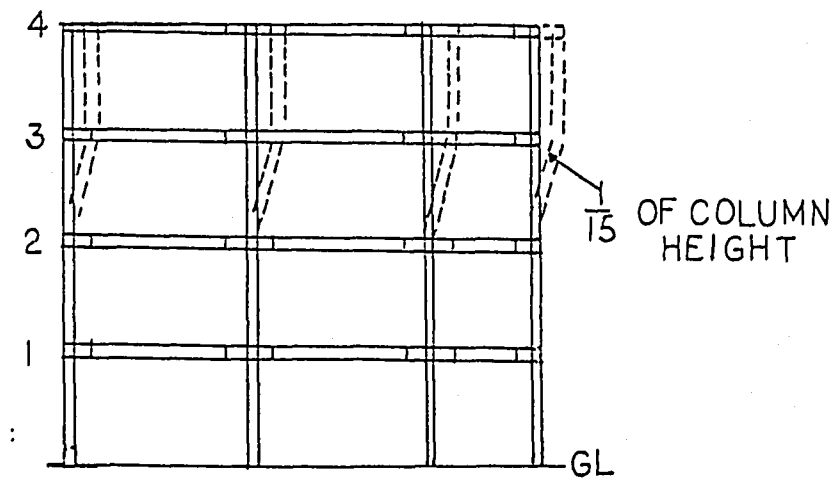
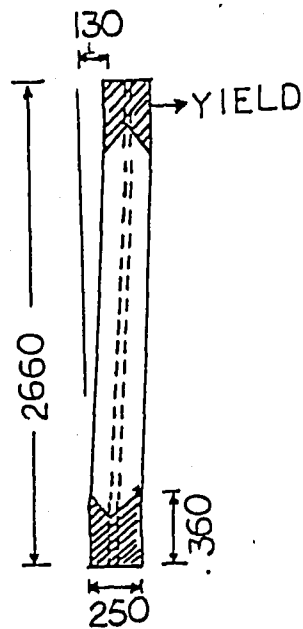


Fig. 5: Damaged Structure after Earthquake



* DIMENSION IN MM

Fig. 6: Deformed Column Shape on the Third Floor

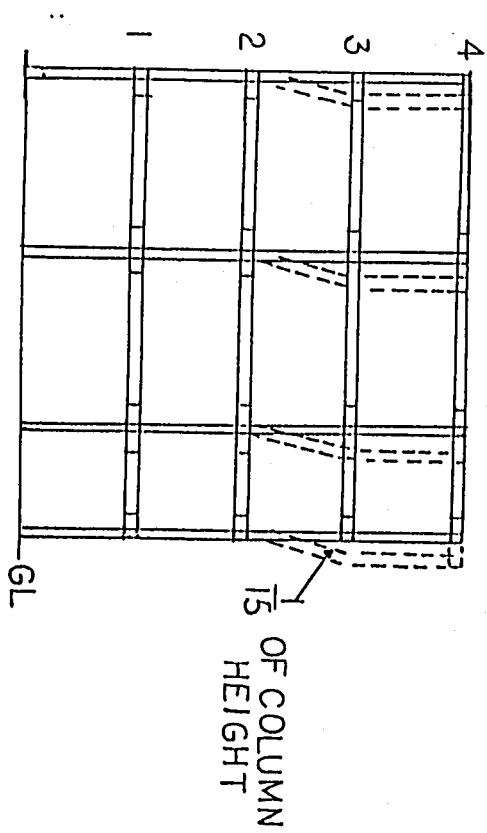


Fig. 5 : Damaged Structure after Earthquake

* DIMENSION IN MM

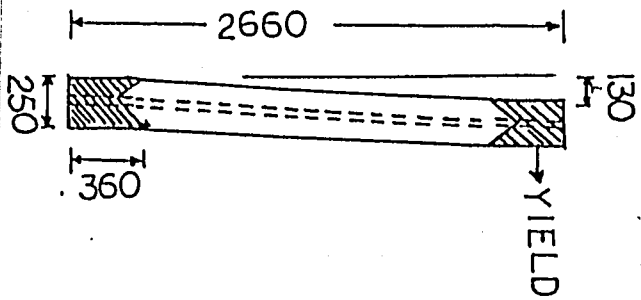


Fig. 6 : Deformed Column Shape on the Third Floor

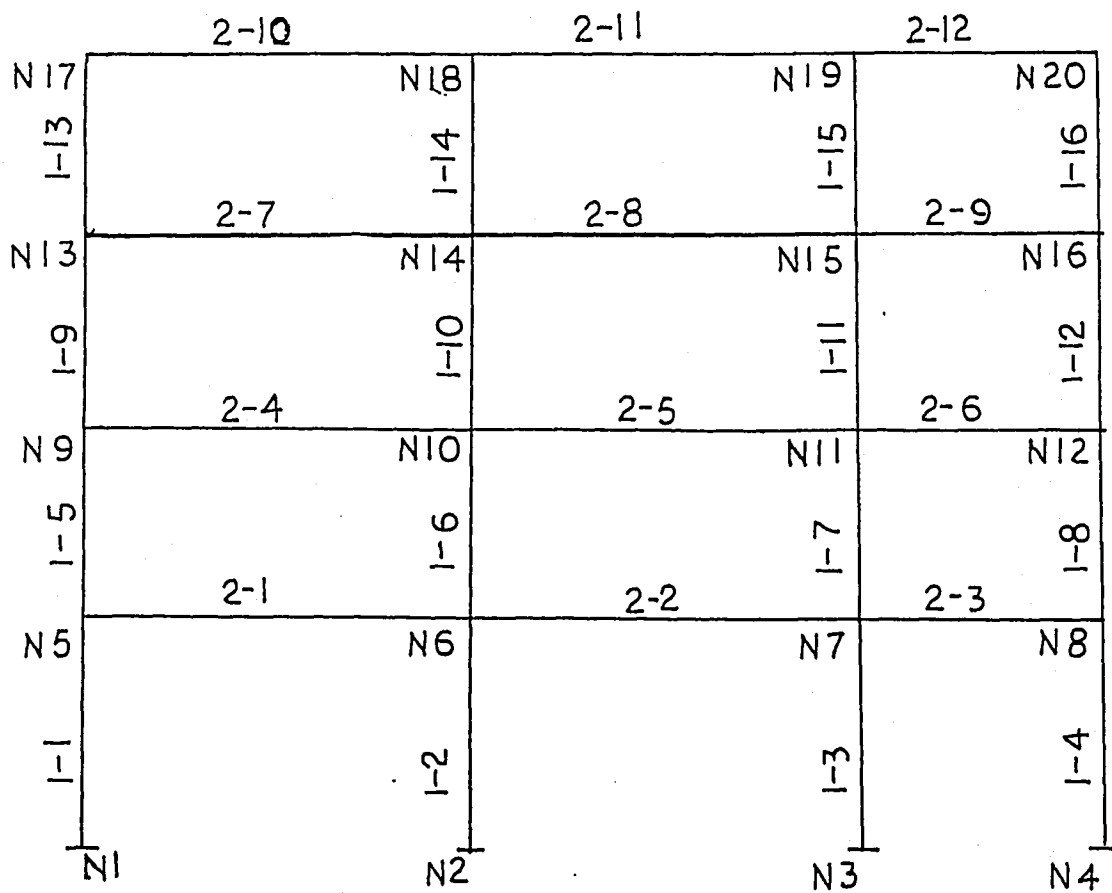


Fig. 7: Node and Element Numbering for SAPIV

	2-10	2-11	2-12	
N17				N20
1-13	2-7	2-8	2-9	1-16
N13	N14	N15	N16	
1-9	0-1	1-1	2-6	1-12
N9	N10	N11	N12	
1-5	1-6	1-7	1-8	
N5	N6	N7	N8	
2-1	2-2	2-3		
1-1	1-2	1-3	4-1	
N1	N2	N3	N4	

Fig. 7: Node and Element Numbering for SAPIV

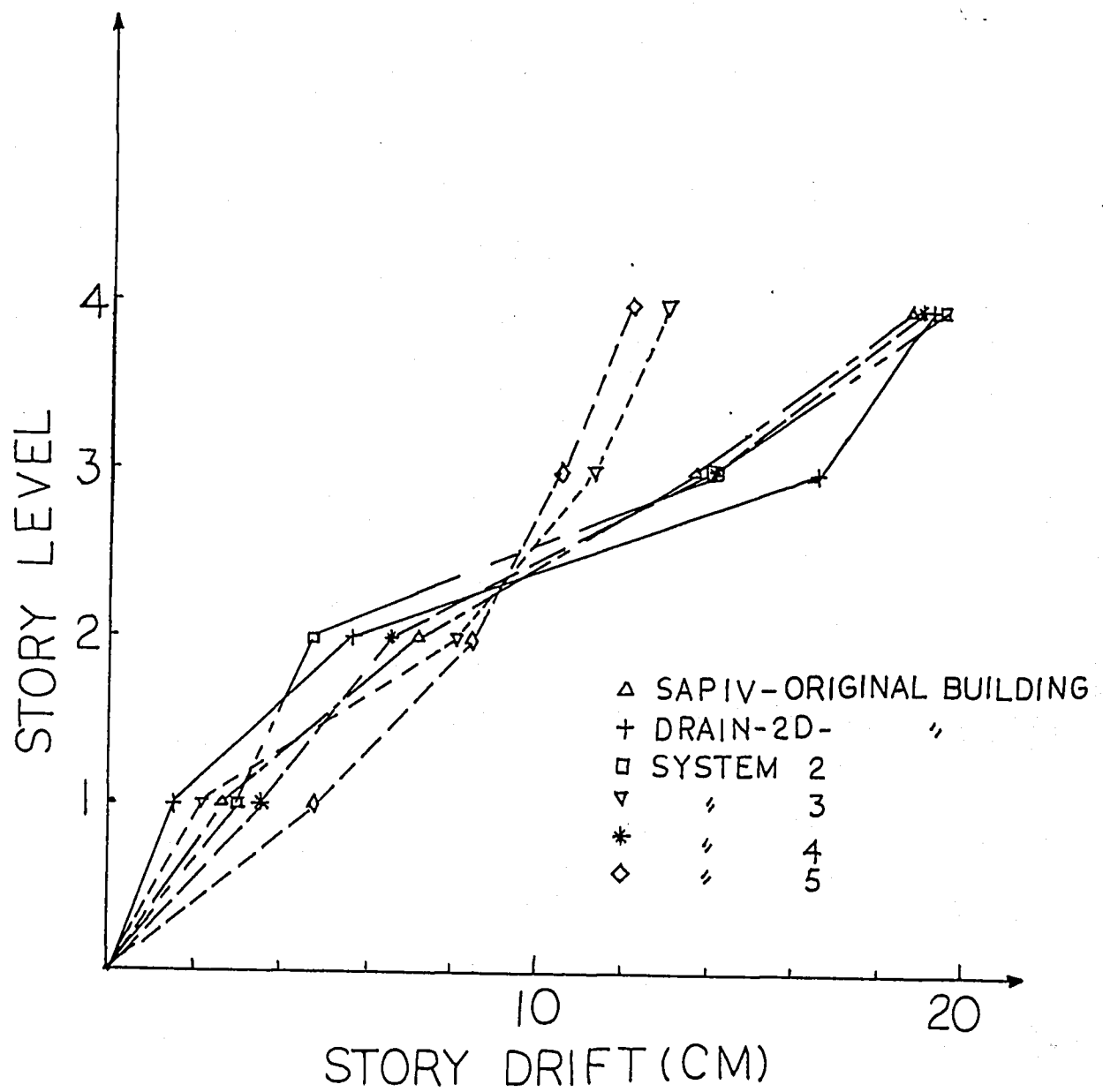


Fig. 8: Maximum Story Drift of Systems in Chapter 2

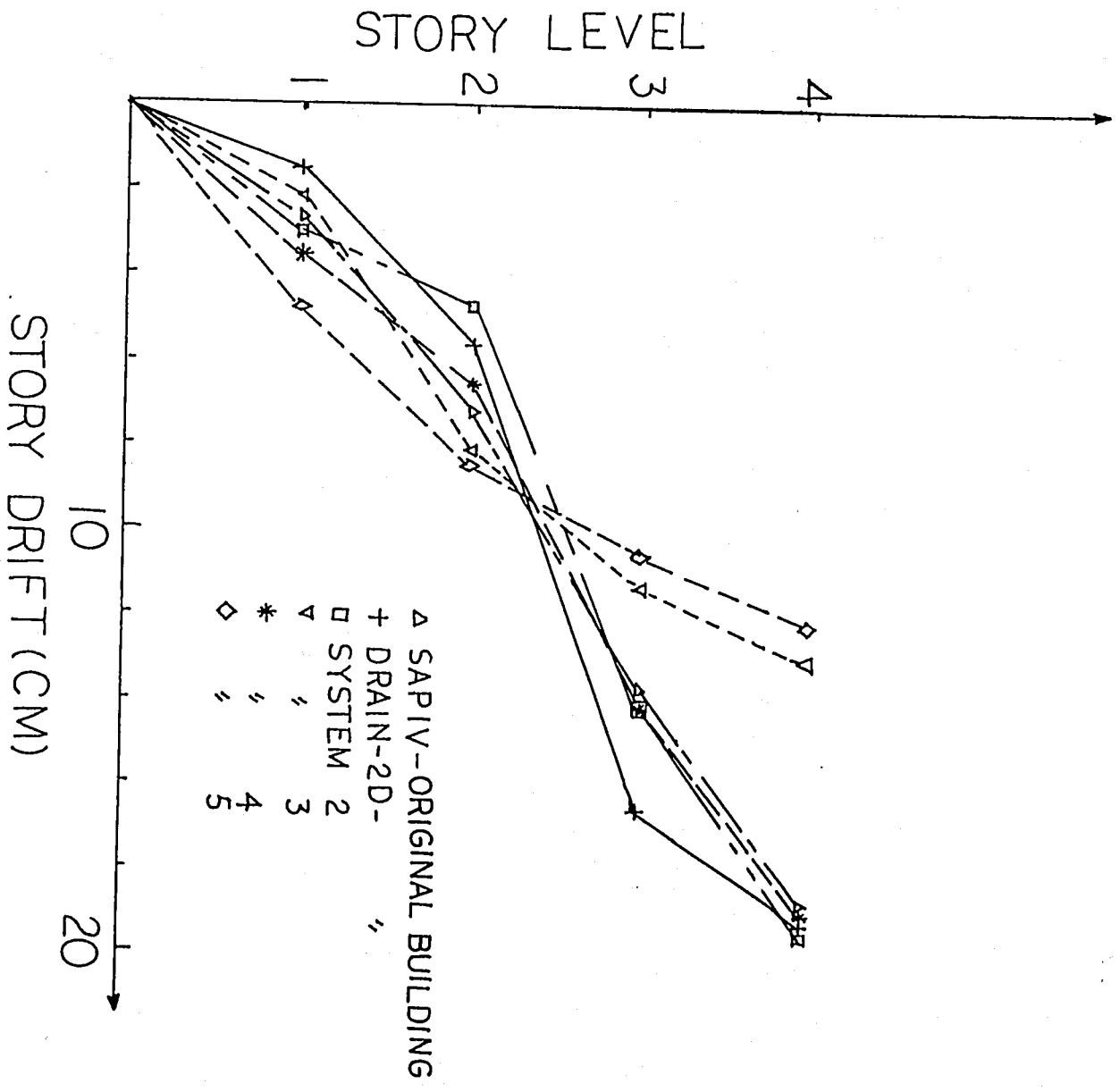


Fig. 8: Maximum Story Drift of Systems in Chapter 2

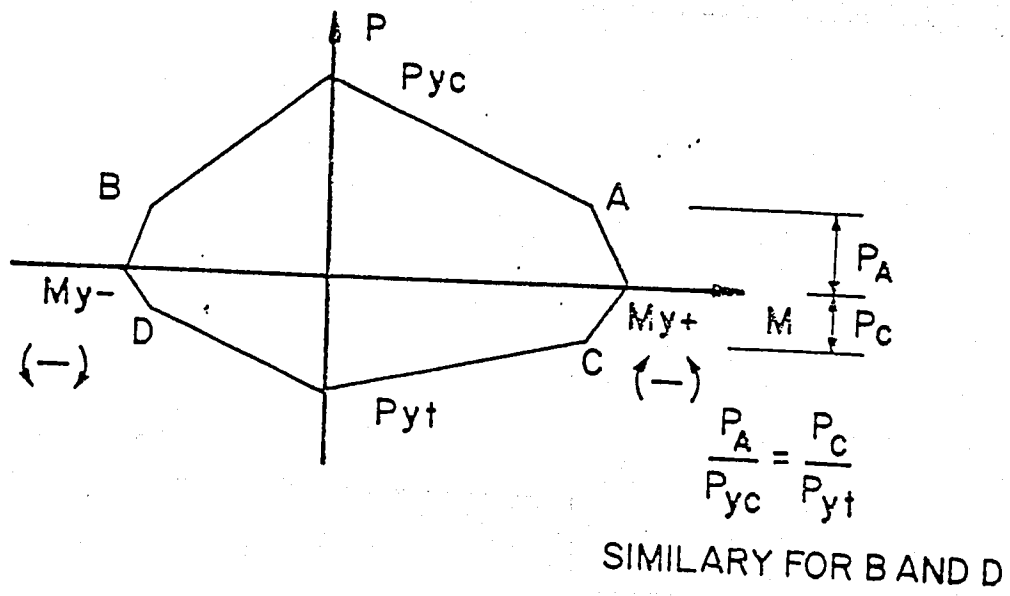
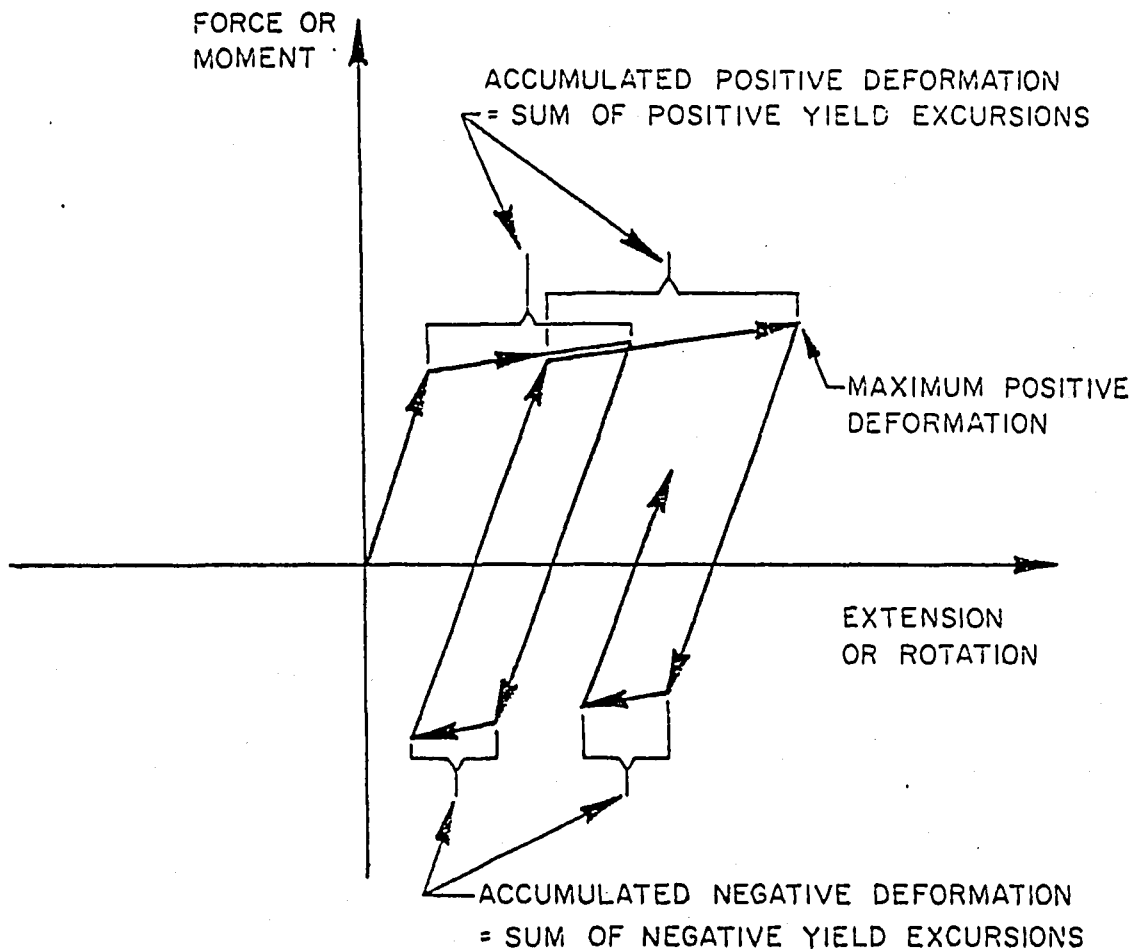


Fig. 9: Yield Interaction Surface for Columns
(Ref. [12])



NOTE THAT MAXIMUM NEGATIVE DEFORMATION
IS ZERO, ALTHOUGH ACCUMULATED NEGATIVE
DEFORMATION IS NOT ZERO

Fig. 10: Procedure for Computation of Accumulated
Plastic Deformation (Ref. [12])

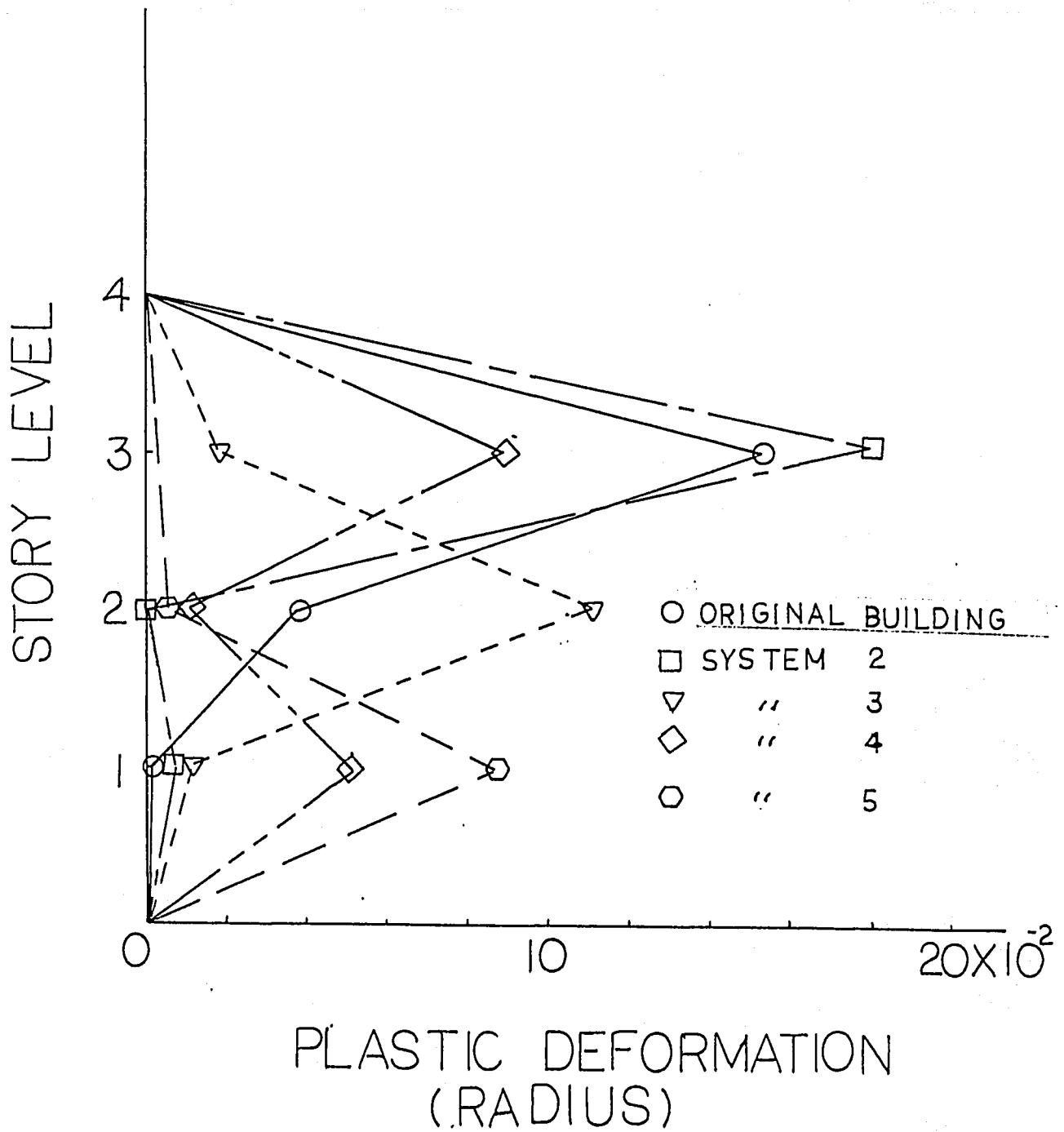


Fig. 11: Maximum Plastic Deformation of the Systems in Chapter 2

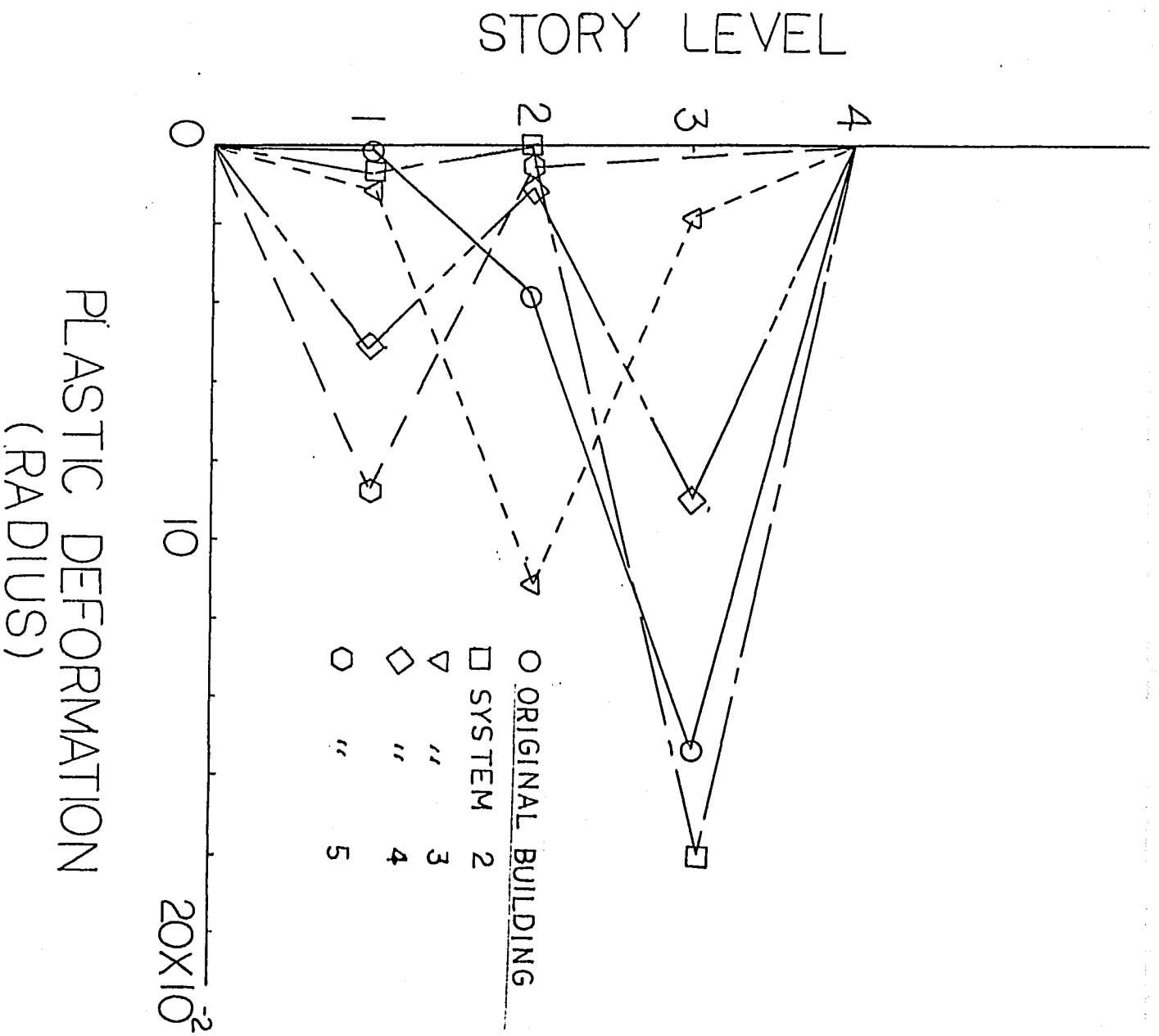
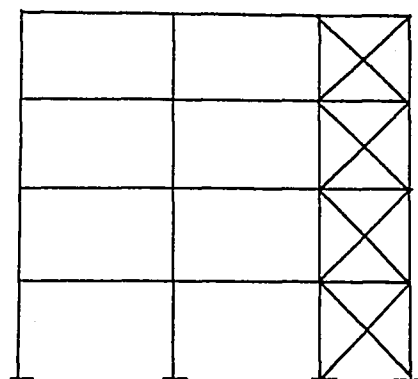
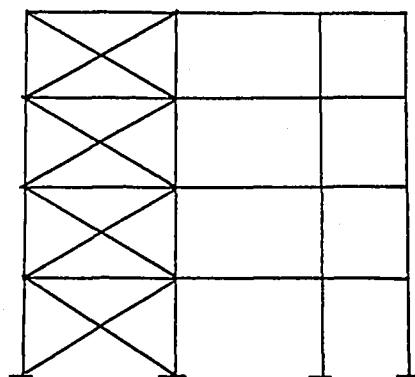


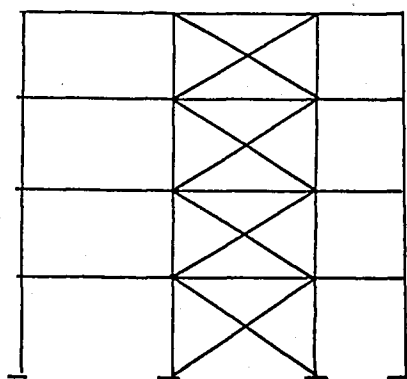
Fig. 11: Maximum Plastic Deformation of
the Systems in Chapter 2



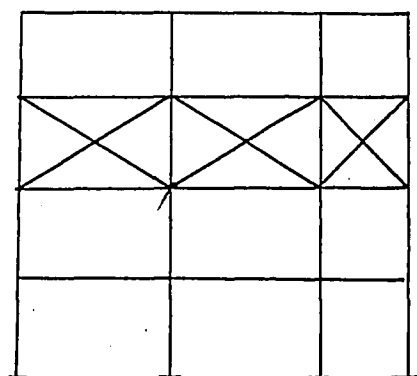
SYSTEM 1



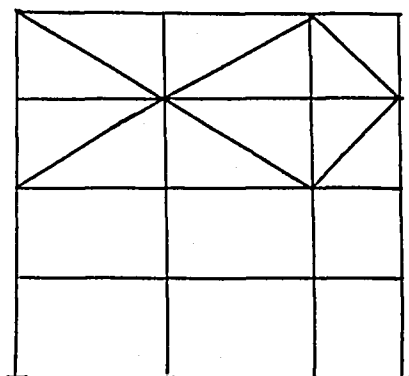
SYSTEM 2



SYSTEM 3



SYSTEM 4



SYSTEM 5

Fig. 12: Different Bracing Arrangement in X-bracing System

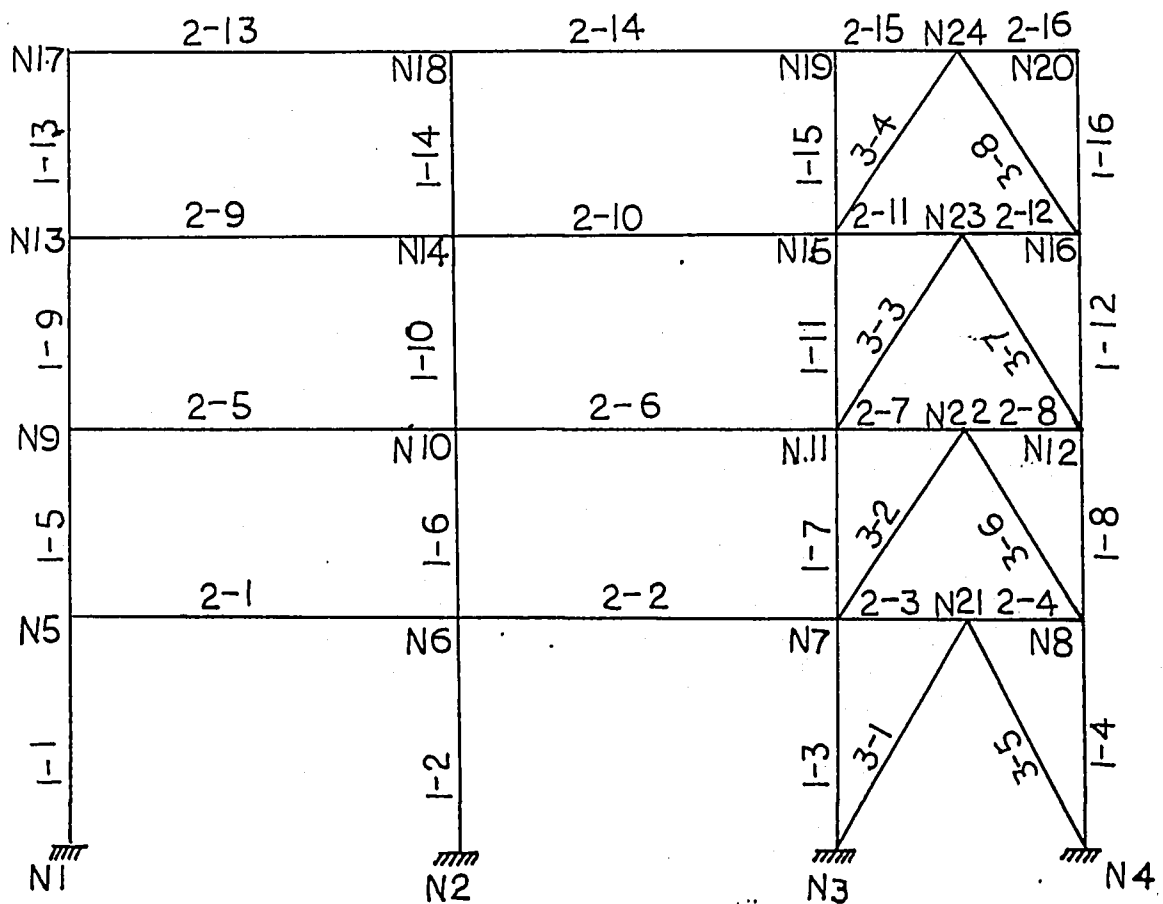


Fig. 13: Node and Element Numbering for Concentrically K-Braced Frames

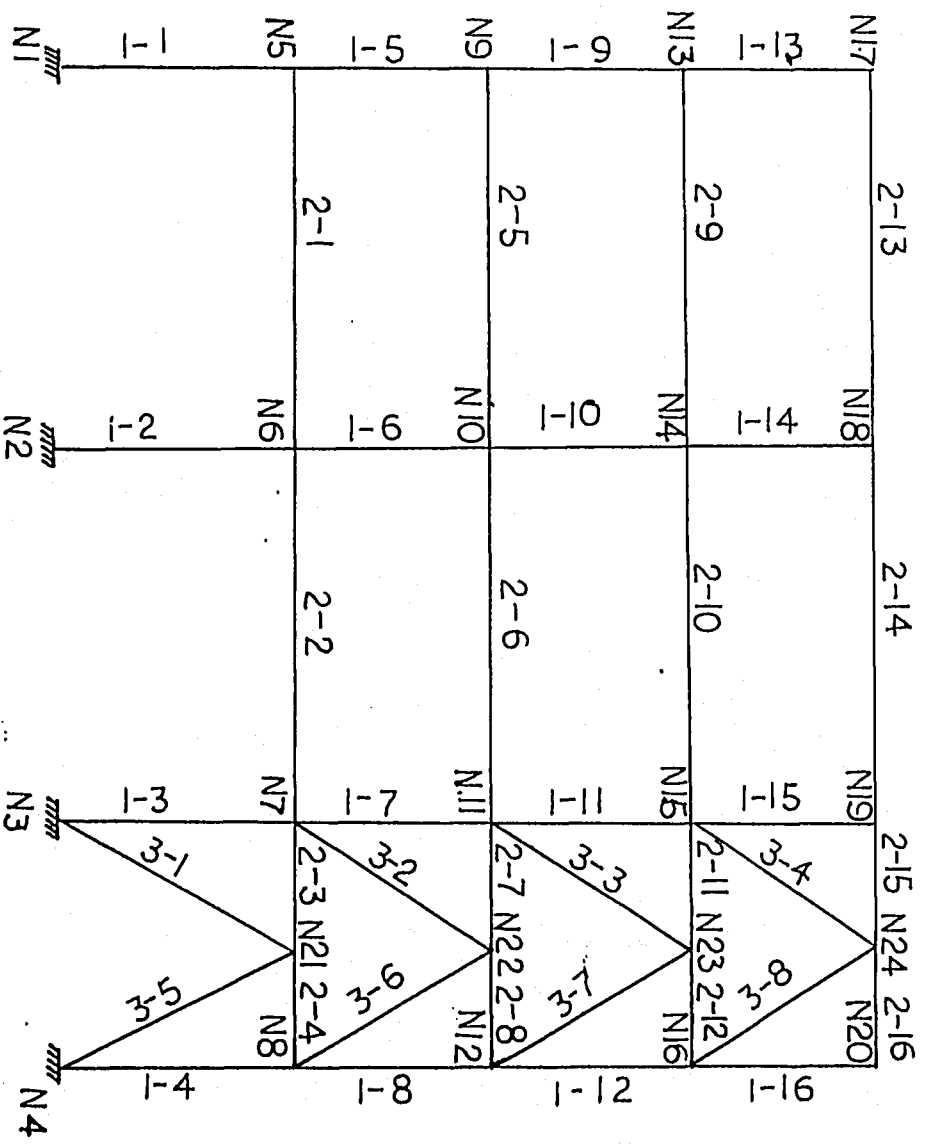


Fig. 13: Node and Element Numbering for Concentrically K-Braced Frames

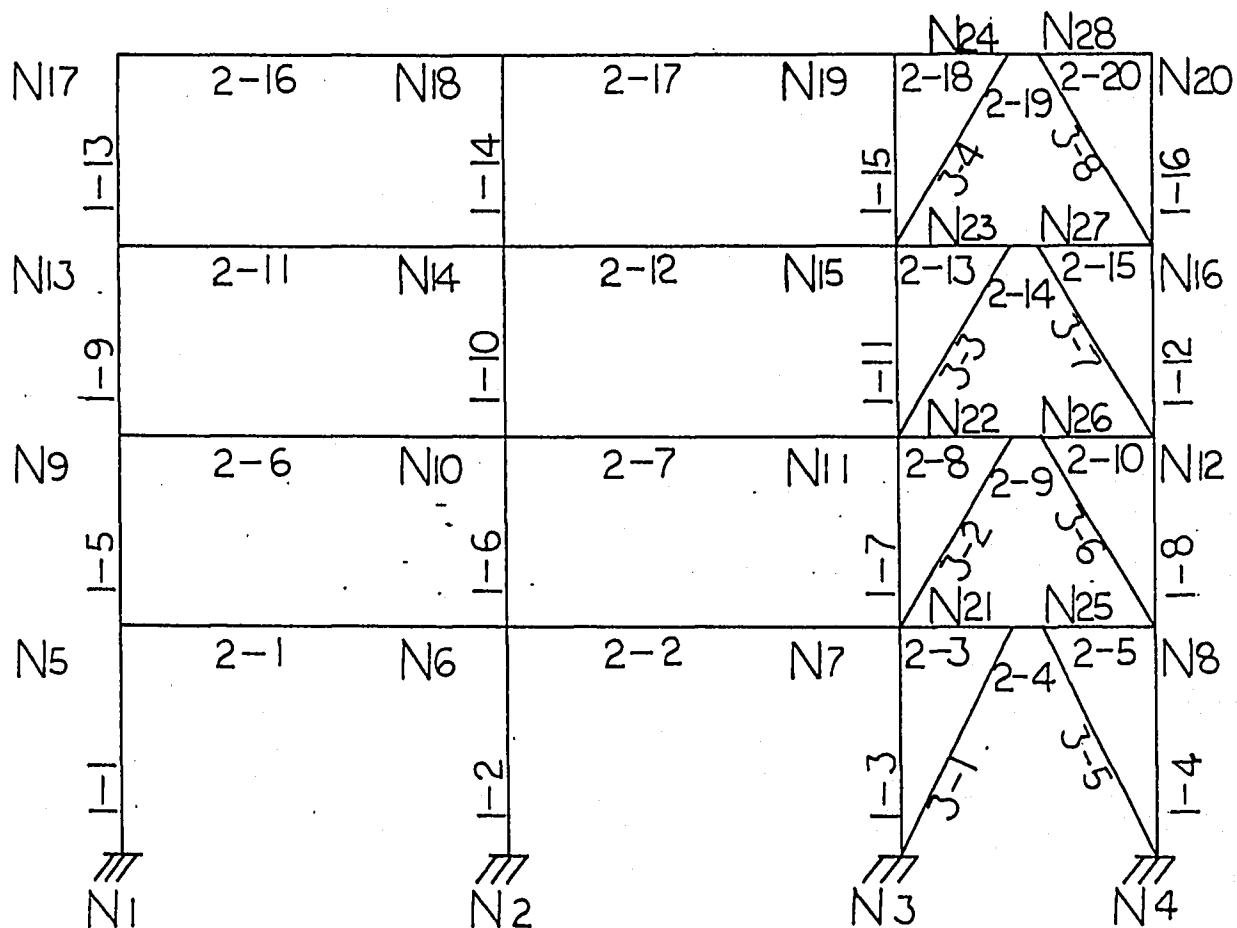


Fig. 14: Node and Element Numbering for Eccentrically K-Braced Frame

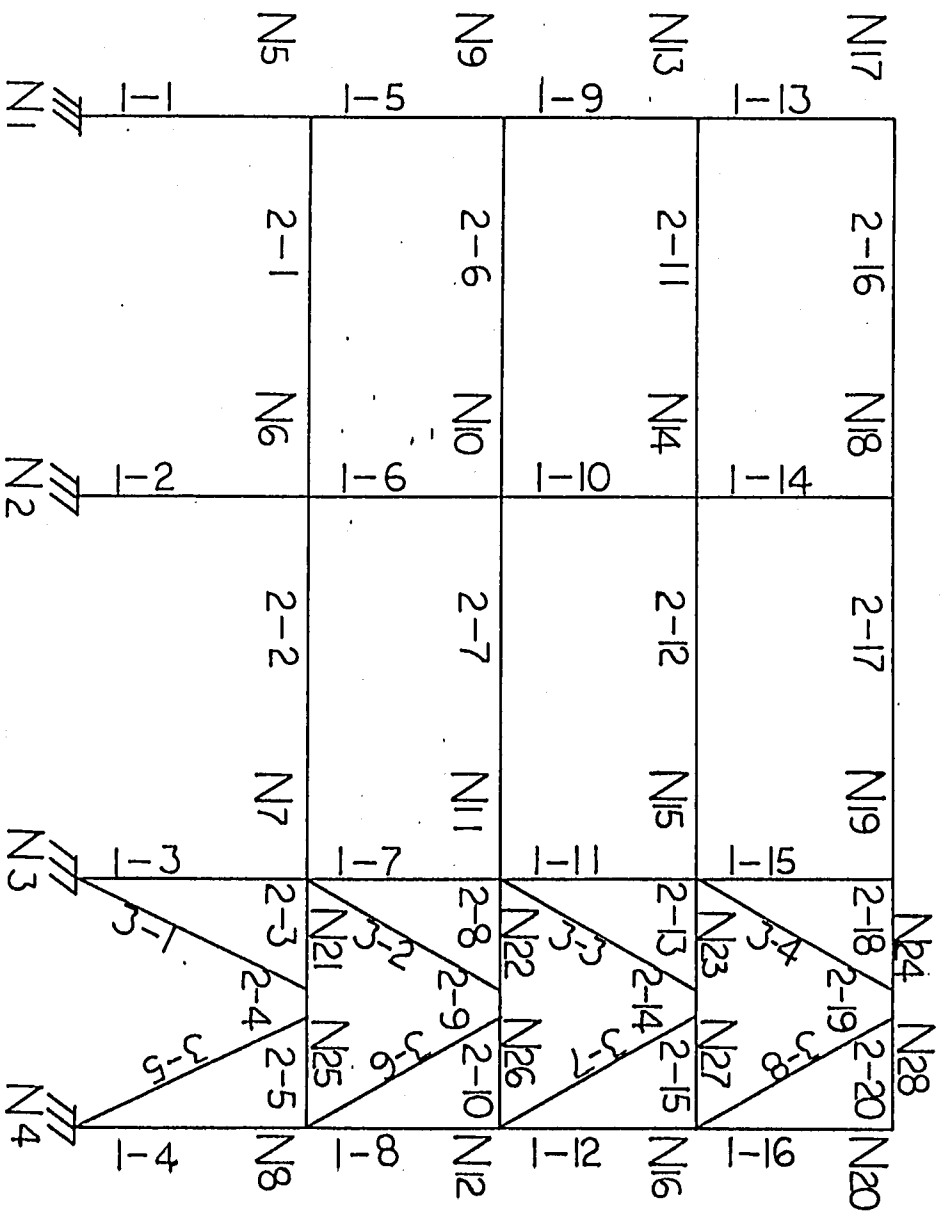


Fig. 14: Node and Element Numbering for Eccentrically K-Braced Frame

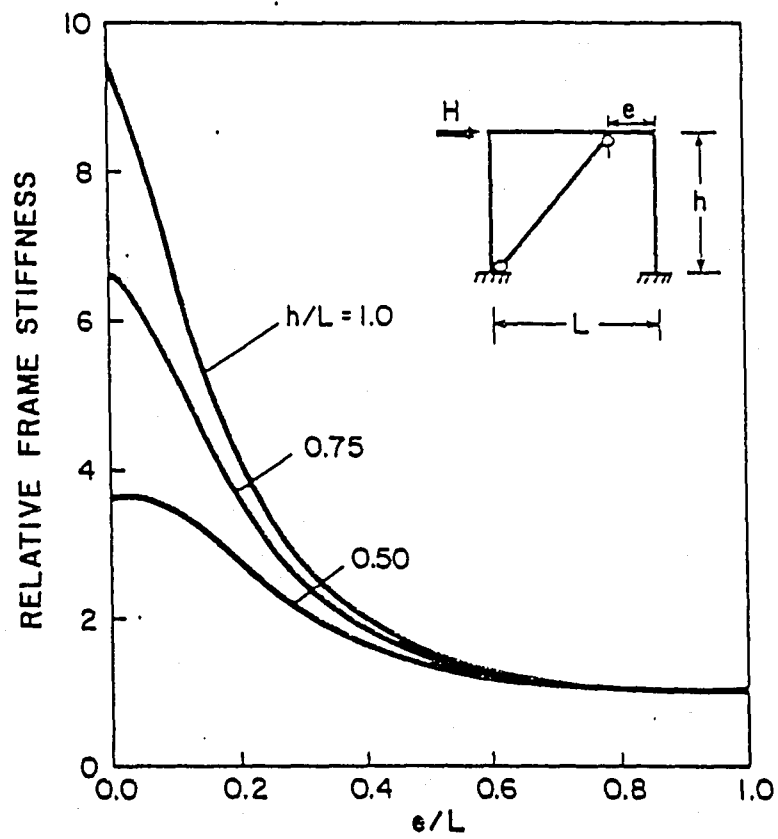


Fig. 15: Variation of Frame Stiffness for Different Eccentricity Ratio (Ref. [6])

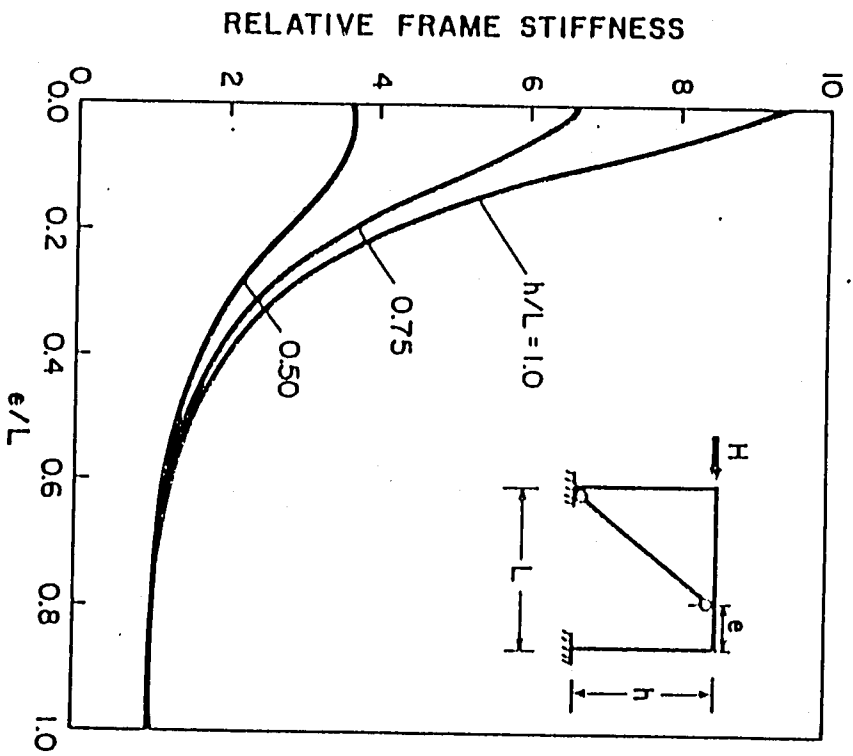


Fig. 15: Variation of Frame Stiffness for Different Eccentricity Ratio (Ref. [6])

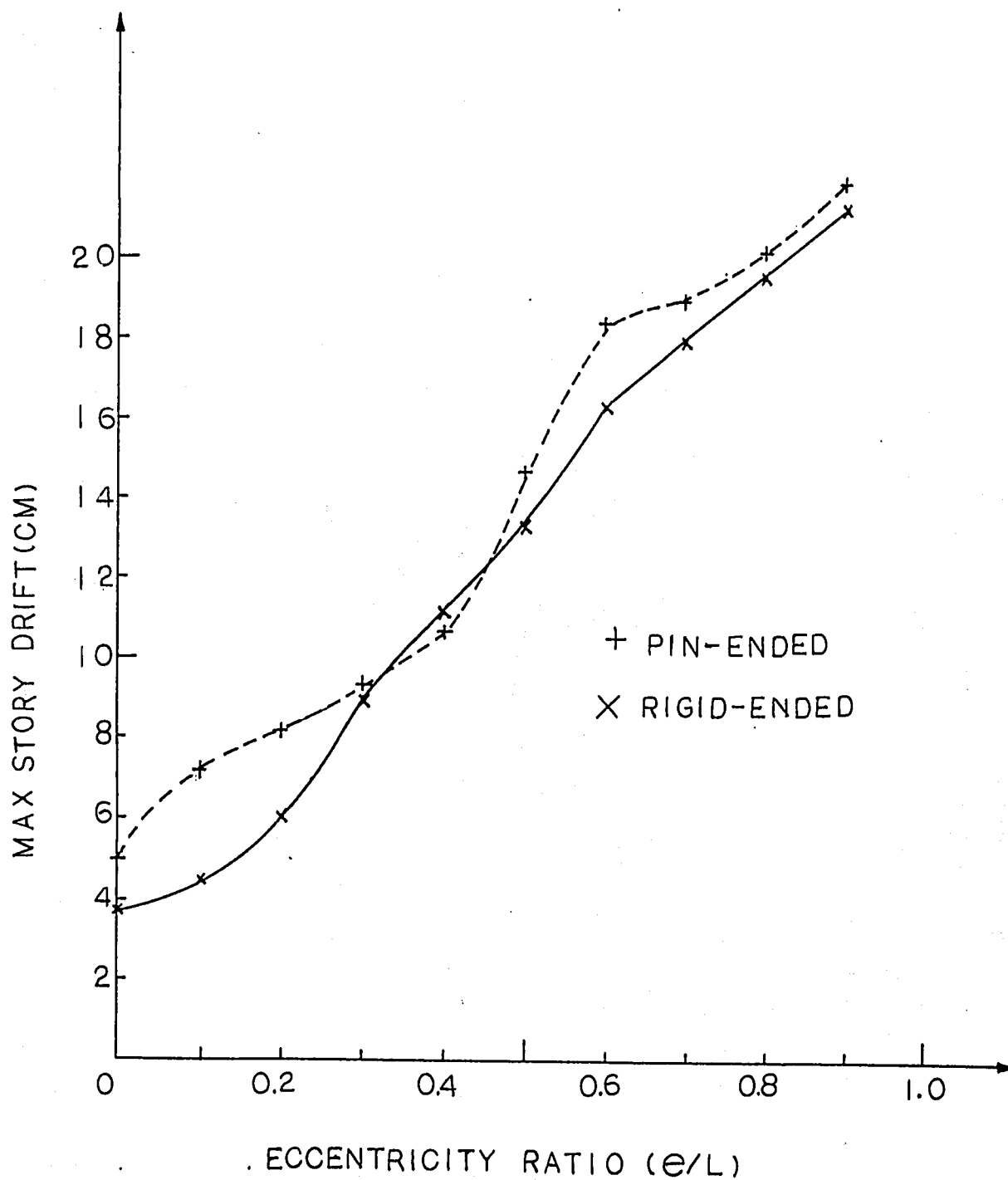


Fig. 16: Maximum Story Drifts of Eccentrically Braced Frames

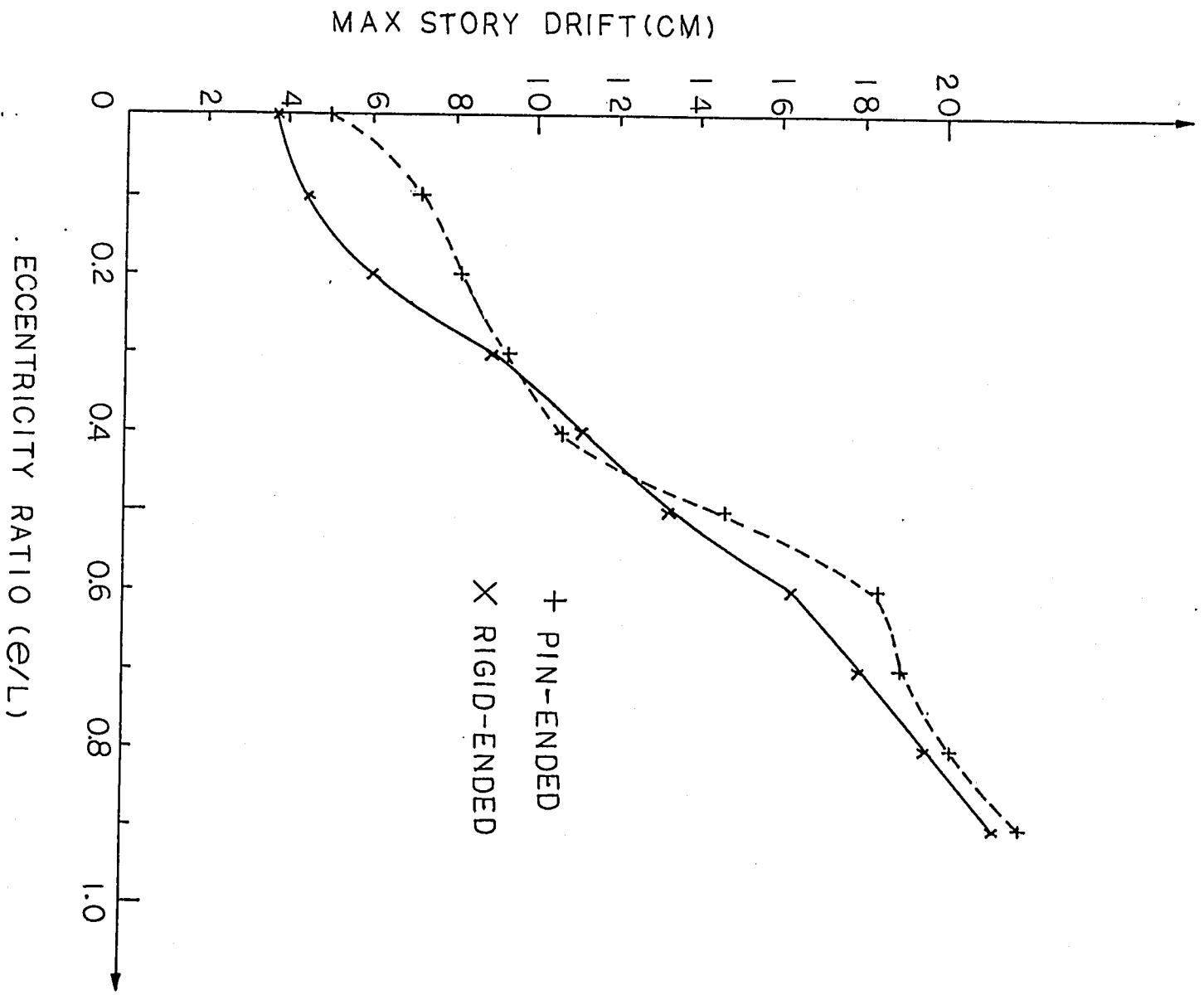


Fig. 16: Maximum Story Drifts of Eccentrically Braced Frames

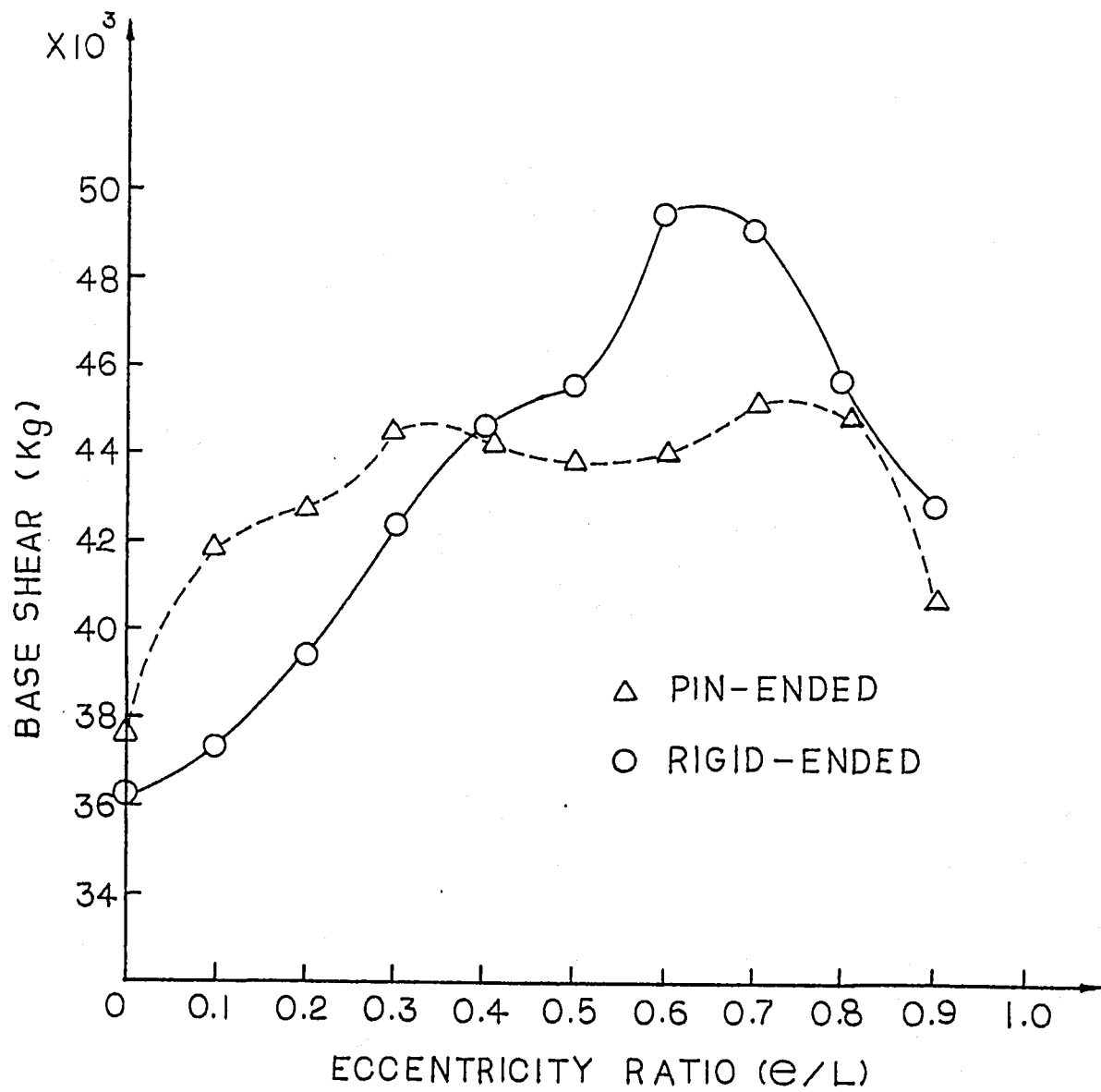


Fig. 17: Base Shear For Eccentrically Braced Frames

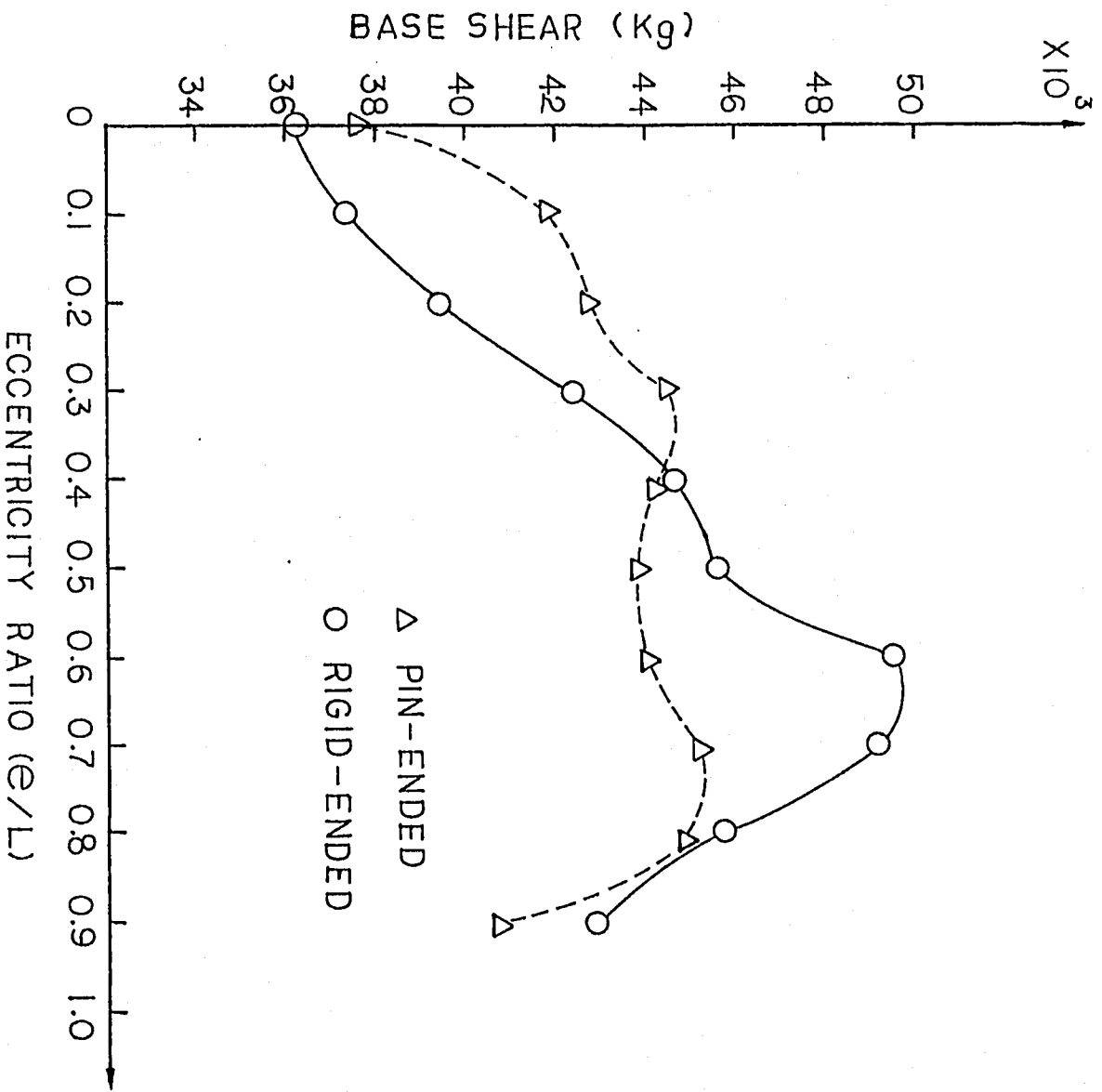


Fig. 17: Base Shear For Eccentrically Braced Frames

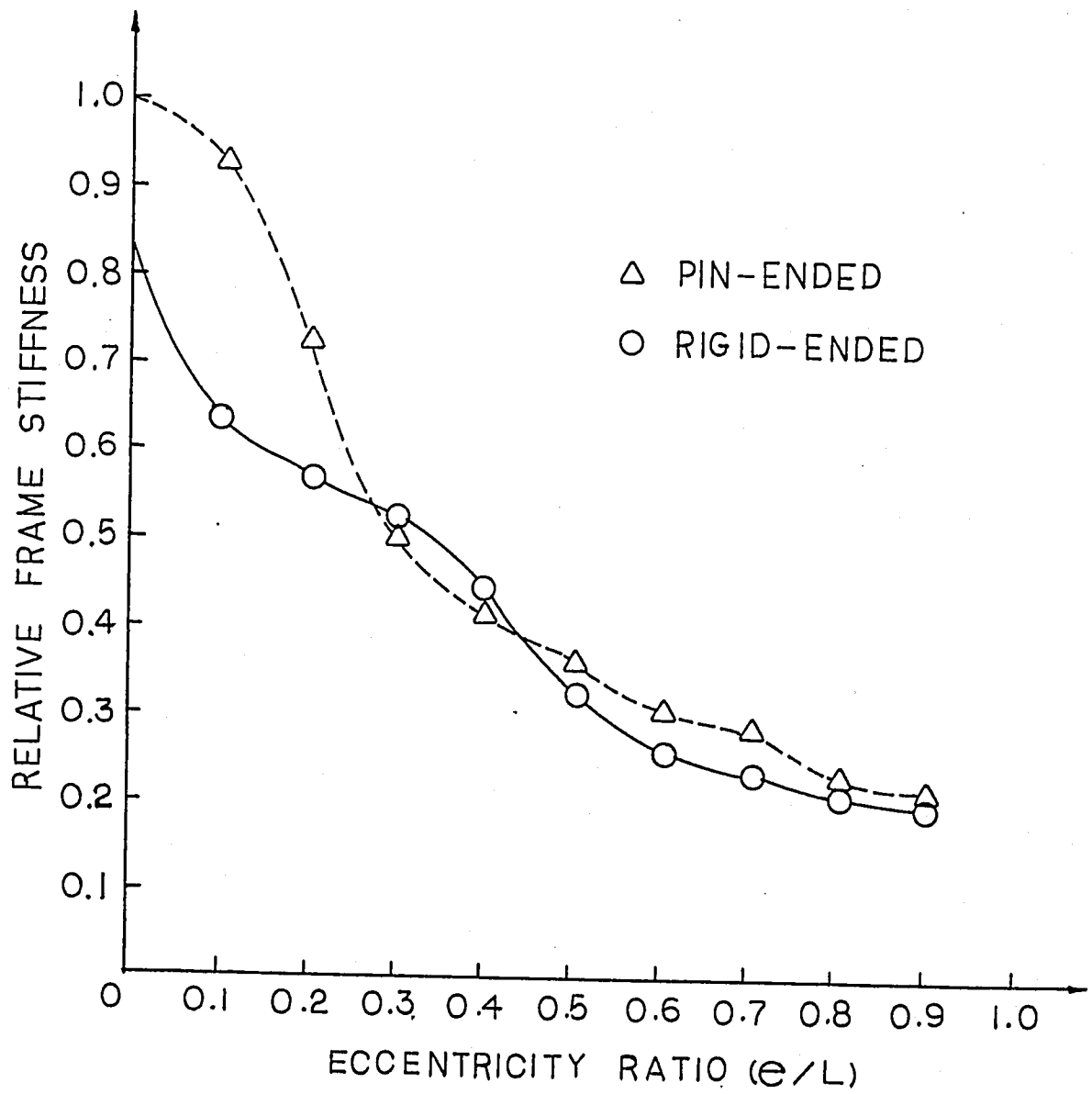


Fig. 18: Variation of Lateral Stiffness for Eccentrically Braced Frames

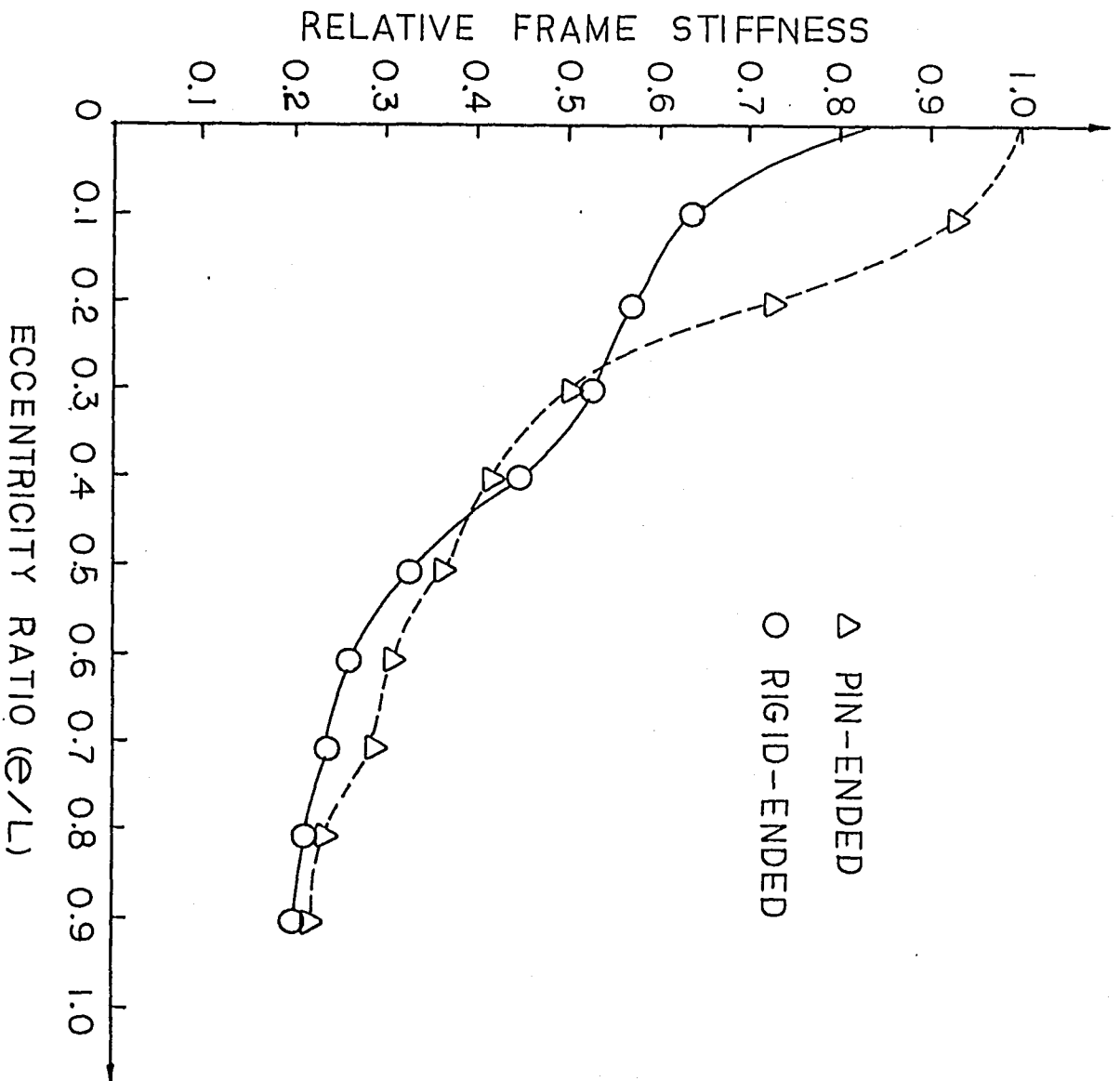


Fig. 18: Variation of Lateral Stiffness
for Eccentrically Braced Frames

REFERENCES

- [1] Architectural Institute of Japan.
Damage Investigation Report on Miyagi Earthquake.
in Japanese.
- [2] AISC.
Steel Construction
8th ed edition, American Institute of Steel
Construction, New York, 1981.
- [3] Architectural Research Institute in Japan
Construction Department.
Damage Report of the Miyagi Earthquake.
Monthly Publication, No.71..
- [4] ASCE.
Plastic Design in Steel -- A Guide and Commentary
2nd edition, ASCE, 1971.
- [5] Bathe, K.J., Wilson, L.E. and Peterson, F.E.
SAP IV -- A Structural Analysis Program for Static
and Dynamic Reponse of Linear System
University of California, Berkeley, California,
1974.
- [6] Hjelmstad, K.D., and Popov, E.P.
Cyclic Behavior and Design of Link Beams.
Reprint SC-7, ASCE Structuree Congress, New Orleans
Oct. 1982.
- [7] Horne, M.R.
A Moment Distribution Method for the Analysis and
Design of Structures by the Plastic Theory.
Proceedings of Institute of Civil Engineers Vol
3(No.1), April, 1954.
- [8] Jain, A. K.
Hysteresis Behavior of Bracing Members and Seismic
Response of Braced Frames with Different
Proportions.
PhD thesis, University of Michigan, July, 1978.

- [9] Jain A.K. and Goel, S.C.
Hysteresis Models for Steel Members Subjected to Cyclic Buckling of Cyclic End Moments and Buckling (User's Guide for DRAIN-2D: EL9 and EL10).
Technical Report No. UMEE73R6 , University of Michigan, December, 1978.
- [10] JSSC Inquiry Commission of Earthquake Damage on Steel Structures.
Reports on the Steel Structure Damage in Miyagi Earthquake.
JSSC, Japan Steel Structure Construction Vol 14(No. 153), September, 1978.
in Japanese.
- [11] Kahn, L.F. and Hanson, R.D.
Inelastic Cycles of Axially Loaded Steel Members.
ASCE Journal of the Structural Division Vol 102,
May, 1976.
- [12] Kanaan, A.E. and Powell, G.H.
DRAIN-2D - A General Purpose Computer Program for the Dynamic Analysis of Inelastic Plane Structures.
Technical Report EERC Report 73-6, University of California, Berkeley, April, 1973.
- [13] Kato, Ben and Akiyama, Hiroshi.
Seismic Design of Steel Buildings.
ASCE J. of Structural Div. (ST8):p1709-1720,
August, 1982.
- [14] Popov, E.P. and Black, R.G.
Steel Structures Under Severe Cyclic Loadings.
ASCE J. Structural Division Vol 107(ST9),
September, 1981.
- [15] Roeder, C. W. and Popov, E.P.
Inelastic Behavior of Eccentrically Braced Steel Frames Under Cyclic Loadings.
Technical Report, University of California, Berkeley, August, 1977.
- [16] Roeder, C. W. and Popov, E.P.
Eccentrically Braced Steel Frames for Earthquakes.
ASCE Journal of the Structural Division Vol 104(ST3):P391-413, March, 1978.

- [17] Seed, H.B. and Idriss, I.M.
Influence of Local Soil Conditions on Building
Damage Potential During Earthquakes.
Technical Report EERC 69-15, University of
California, Berkeley, December, 1969.
- [18] Steel Material Club.
Damages of the Steel Structures by Earthquake, Wind
and Snow.
in Japanese.
- [19] Toshio Shiga, Akenori Shibata, Junichi Shibuya and
Junichi Jakahashi.
Observations of Strong Earthquake Motions and
Nonlinear Response Analyses of the Building of
Architectural and Civil Engineering Department,
Tohoku University.
Technical Report Paper No. 301, AIJ, March, 1980.
in Japanese.
- [20] Uniform Building Code
International Conference of Building Officials,
Whittier, CA, 1976.

VITA

Shiunn-Jang Wang, born August 5, 1957 in Taipei, Taiwan, R.O.C, is the son of San-Ching Wang and Yen-Yin Ding.

After graduating from National Taiwan University, where he got his B.S. degree in civil engineering, he served two years in Chinese Marine Corps as an logistic officer.

Mr. Wang came to Lehigh University on August 1981 for his M.S. degree. He has been employed as a research assistant in the Fritz Engineering Laboratory, where he has been associated with the project "Earthquake Resistance of High-Rise Buildings Systems". He has also been involved with the work of the Council on Tall Buildings and Urban Habitat, which is headquartered at Lehigh.